Faster Gates for Quantum Computing and Simulation in Circuit QED

Géraldine Haack

Munich 2008

Faster Gates for Quantum Computing and Simulation in Circuit QED

Diploma Thesis

presented by

Géraldine Haack

Lausanne, the 1. of February 2008

ÉCOLE POLYTECHNIQUE
FÉDÉRALE DE LAUSANNE

LMU

First supervisor: Prof. Enrique Solano (LMU)
Second supervisor: Dr. Florian Marquardt (LMU)
Evaluators: Prof. Enrique Solano (LMU) and Prof. Dmitri Ivanov (EPFL)

Contents

Abstract

Circuit quantum electrodynamics (Circuit QED) is a novel field combining quantum-optical cavity QED concepts with solid-state devices, where superconducting qubits are coupled to microwave resonators. The fundamental dynamics in Circuit QED is associated with the Jaynes-Cummings model, well known in quantum optics, describing the interaction between a two-level system with a single mode of a cavity field. While current experiments focus on single-qubit single-resonator devices, recently a two-dimensional cavity architecture has been proposed for standard quantum computing, where qubits are placed at the crossings of a two-dimensional cavity array.

Taking into account the constraints and advantages of the newly suggested Circuit QED setup, we will study the implementation of universal one- and two-qubit operations such as Hadamard, CPHASE, and iSWAP gates, based exclusively on resonant interactions. The latter can be obtained due to a suitable utilization of three-level physics in our extended Circuit QED approach. Though two-qubit gates working in the off-resonant regime are widely considered, they are slow when compared to the proposed resonant ones. Exploiting these engineered fast operations, we will also present an optimized protocol for the implementation of a two-dimensional cluster state, a key requirement for one-way quantum computing. Finally, we will use similar tools to discuss possible simulations of strongly correlated systems, such as the XX and Ising models in Circuit QED.

Zusammenfassung

Schaltkreis-Quantenelektrodynamik (Circuit QED) ist ein neues Feld, welches bekannte Konzepte der Cavity QED mit Aufbauten aus der Festkörperphysik kombiniert: supraleitende Qubits sind an Mikrowellenresonatoren gekoppelt. Die fundamentale Dynamik der Wechselwirkung wird durch das Jaynes-Cummings Model beschrieben. Dieses ist ein bekanntes Modell aus der Quantenoptik, um die Wechselwirkung von einem Zwei-Niveau-System mit einem Laserfeld zu beschreiben. Während momentan der experimentelle Fokus noch auf Systemen bestehend aus einem Resonator und einem Qubit liegt, gibt es theoretische Vorschläge für zweidimensionale Architekturen, in denen die Resonatoren in Gitterstrukturen angeordnet sind, und die Qubits an den Kreuzungspunkten plaziert werden. In dieser Diplomarbeit werden wir mit diesem Gitter arbeiten und die Vor- und Nachteile dieser Struktur für die Ausführung von Operationen berücksichtigen.

Im ersten Teil werden wir die Implementierung von universellen ein und zwei Qubits Operationen, wie die Hadamard, CPHASE und iSWAP Transformation behandeln. Unter Zuhilfenahme des Resonators als Mediator und einem dritten Anregungszustand des Qubits können wir diese Operationen auschliesslich durch resonante (d.h. schnelle) Prozesse verwirklichen. In einem zweiten Teil werden wir diese neuen schnellen Operationen für die Entwicklung des quantum computing ansetzen. Zuerst präsentieren wir ein Protokoll zur Konstruktion eines Clusterzustandes. Dieser spezielle verschränkte Mehrteilchenzustand findet Anwendung im One-way Quantencomputer. Als zweite und letzte Anwendung werden wir die Ausführung von Operationen im resonanten Regime in Circuit QED vorstellen, die stark korrelierte Modelle wie das XX- oder Ising-Modell simulieren können.

Résumé

L'électrodynamique quantique en circuit (Circuit QED) est un domaine de recherche récent où des concepts de l'électrodynamique quantique en cavité sont appliqués à des systèmes de la physique du solide: des bits quantiques superconducteurs (superconducting qubits) couplés à des résonateurs micro-ondes. La dynamique fondamentale de cette interaction peut être comprise grâce au modèle de Jaynes-Cummings qui décrit l'interaction entre un système atomique à deux niveaux avec un mode du champ de cavité en optique quantique.

Les expériences actuelles en électrodynamique quantique des circuits se font généralement avec des systèmes composés d'un bit quantique superconducteur et d'un résonateur. Néanmoins des propositions théoriques concernant la fabrication des qubits et l'architecture des résonateurs émergent afin d'améliorer la cohérence des systèmes et de pouvoir mettre en oeuvre des algorithmes, dans le but du calcul quantique conventionnel par exemple. Une des nouvelles architectures proposées est une grille de résonateurs à deux dimensions où les qubits superconducteurs sont placés à l'intersection de deux cavités. Par exemple, nous utiliserons ce cadre pour réaliser des états intriqués à plusieurs qubits, ce qui mettra en évidence les avantages et inconvénients de cette architecture plus complexe.

Dans une première partie, nous étudierons la mise en oeuvre d'opérations à un et deux qubits superconducteurs telles que les portes Hadamard, CPHASE et ISWAP, toutes étudiées exclusivement dans le régime résonant. Elles constituent les briques des ensembles de portes "universelles". Le régime permet de réaliser des interactions à une vitesse rapide comparée à celle obtenue dans un régime non-résonant ou dispersif. Néanmoins la réalisation de toutes les portes dans ce régime nécessite l'utilisation de la cavité comme médiateur ainsi qu'un qubit superconducteur à trois niveaux. Cette dernière condition n'est pas triviale et nous discuterons de sa justification. Dans une seconde partie nous nous appliquerons à utiliser ces nouveaux outils pour le développement du calcul quantique en électrodynamique en circuit. Nous proposerons un protocole optimisé dans le temps pour mettre en oeuvre un cluster en un temps optimisé. Ce cluster est un état intriqué requis lors de la réalisation d'un ordinateur quantique particulier (a one-way quantum computer). Enfin nous présenterons la réalisation d'opérations non-triviales en régime résonant permettant de simuler en électrodynamique quantique des circuits des systèmes fortement corrélés tels que le modèle XX ou le modèle d'Ising dans un champ magnétique transverse.

Chapter 1

Circuit Quantum Electrodynamics

Circuit quantum electrodynamics (Circuit QED) is a novel subject of interest in the field of solid-state quantum computation. It appeared from the association of quantum optical cavity QED with macroscopic quantum mechanics. On the one hand quantum mechanics is commonly associated with microscopic particles like atoms or photons. Thermal motion masks quantum fluctuations and thus quantum behaviors can usually not be observed in macroscopic objects. However there exist several physical systems where a large number of microscopic particles is described by a macroscopic wave function described with the tools of classical mechanics. However one can observe behaviours only interpretable with quantum mechanics. This is the case for instance in the Bose-Einstein condensation or in superconductivity where a macroscopic fraction of the electrons are in the superconducting state and can be described by a macroscopic wave function Ψ [1].

On the other hand Cavity QED with concepts of quantum optics is a large research field where people study the interaction between few atoms and few photons [2]. In the case of one atom and a discrete electromagnetic mode of a cavity field, the interaction is modeled by the Jaynes-Cummings Hamiltonian. For instance, the strong coupling regime required to observe the exchange of energy described in the Jaynes-Cummings Hamiltonian has been reached [3, 4] and could be exploited in quantum information or quantum communication.

Solid-state quantum computation and more specifically Circuit QED can be considered as a new approach to Cavity QED. The idea is to simulate the fundamental interaction of an atom and a mode of the cavity field at a microscopic scale and not anymore at an atomic scale. The system is composed of superconducting qubits (SCqubits) built with the physics of Josephson junctions, in which quantum macroscopic effects can be observed, and microwave resonators ([5] - [7]) . Some others subjects of interest like trapped ions ([8], [9]), quantum dots [10] or semiconductor spin qubits [11] aim at observing this interaction at microscopic and mesoscopic scales.

Circuit QED is an efficient architecture for solid-state quantum computing in which superconducting qubits considered as artificial atoms interact with modes of microwave resonators playing the role of cavities. It has been shown, and we will derive it in a more general frame in this chapter, that the fundamental Hamiltonian describing the dynamics of Circuit QED is equivalent to the Jaynes-Cummings model [12].

Circuit QED has some advantages over previous proposals such as ions in atomic physics and spins in mesoscopic physics because superconducting qubits are macroscopic systems and thus

easier to construct and to couple. Nevertheless, their readout is difficult and they are hard to isolate due to their size, they interact more with the environment. The decoherence of the system is therefore a major issue of circuit QED and the new devices and implementation of quantum circuits have to deal with this important constraint.

In this chapter we will also present a description of the actual realized devices by the leading experimental groups in Yale, Delft and Santa Barbara. Moreover, we will detail the steps to make the analogy between Circuit QED and Cavity QED by deriving the Jaynes-Cummings Hamiltonian describing the interaction between a two-level system and a cavity.

1.1 Elements of Circuit QED

The physical system used in Circuit QED is composed of a superconducting two-level system playing the role of an artificial atom and an on-chip cavity-resonator, usually a superconducting transmission line resonator. There exists several kinds of SCqubits as well as different proposals for the architecture of the cavity. We will now expose briefly possibilities to reproduce in a solid-state system the model of Cavity QED. Some of them exist already and others are still theoretical proposals. We will explain the main characteristics of each of them, a general idea of their functioning and disadavantages [13].

1.1.1 Superconducting qubits

All superconducting qubits are built with one or several Josephson junctions. Therefore their basic physics belongs to the field of superconductivity. The Josephson junctions act as nonlinear inductors in a circuit and thus provide an anharmonicity between the energy levels. They are characterized by two key parameters which determine their behaviour, the charging energy E_C and the Josephson or coupling energy E_J. Their expression will be given later when we will derive the Hamiltonian of Circuit QED. The phase difference of a Josephson junction ϕ in the macroscopic wavefunction of all Cooper pairs and the number N of Cooper pairs on the island are conjugate variables in analogy to the position and momentum in quantum mechanics. They satisfy a relation of the form of the Heisenberg uncertainty relation, $\Delta N \Delta \phi \geq 1$.
There are four different ways of making a qubit with Josephson junctions. They depend in which regime they are realized, which can be distinguished by the different values of the ratio E_J/E_C. The charge qubit works in the charge regime $E_C \gg E_J$ where the number N of Cooper pairs on the island is well defined and the phase ϕ has strong fluctuations. The flux, phase and transmon qubits operate in the flux regime $E_C \ll E_J$ in which the phase ϕ is well defined and the charge N fluctuates strongly. Another key point of all qubits is their characteristic times T_1 and T_2. T_1 stands for the relaxation time of the qubit from its excited level to its ground level and T_2 corresponds to the coherence time, it denotes the time after which the qubit is not anymore isolated from its environment. The coherence time T_2 is a crucial issue for each qubit and we will give its value in addition to the description of each SCqubit.

1) The charge qubit

This qubit is experimentally built and tested in the groups of Yale, Saclay, Chalmers and at the Nippon Electronics Corporation (NEC). It is characterized by:

- $E_J \approx E_C$

- Size: $0.01 \mu m^2$

- Energy-level difference between the two lowest states: 10 GHz
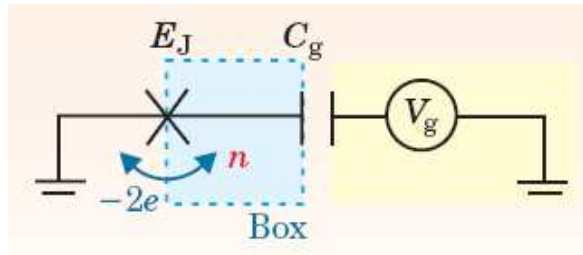
- Coherence time: $T_2 = 0.1 - 1 \mu s$

Figure 1.1: The charge qubit. A Cooper pair box (CPB) or island is driven by a voltage source V_g through a gate capacitance C_g. Cooper pairs with charge $-2e$ in the island can then tunnel from the CPB to the wire through a Josephson junction. Under some assumptions on the different parameters, the CPB is equivalent to a two-level system with states $|0\rangle$ and $|1\rangle$ corresponding to 0 or 1 charge in the CPB. Illustration taken from [13].

Although the charge qubit works theoretically in the charge regime defined by $E_C \gg E_J$, the actual experimental charge qubits work with $E_J \approx E_C$. But the predicted physics of its functioning is the same. The charge qubit is constituted of a small superconducting island, the Cooper pair box (CPB) coupled to the environment by a weak Josephson junction and driven by a voltage source V_g through a gate capacitance C_g. When the box's offset charge induced by the gate voltage is about the same as the charge of a single electron, only two charge states matter: $|0\rangle$ and $|1\rangle$, which have either zero or one extra Cooper pair in the box and are a possibility for the basis states for a qubit. The Cooper pair box is thus described by a two-level quantum system. Regarding the decoherence feature, the main disadvantage of the charge qubit is its big sensitivity to the charge noise. This reduces strongly T_2 and thus the performance of this qubit.

2) The flux qubit

This qubit is experimentally built and tested in the groups of Delft, Berkeley, at the IBM laboratory and the Walter-Meissner Institute (WMI) [14]. It is characterized by:

- $E_J \approx 10^2 E_C$

- size: $0.1 - 1 \mu m^2$

- Energy-level difference between the two lowest states: 10 GHz
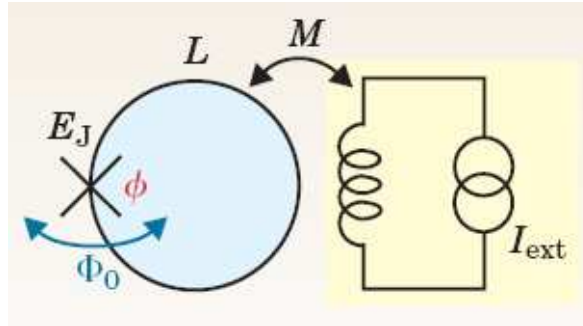
- Coherence time: $T_2 = 1 - 10 \mu s$

Figure 1.2: The flux qubit. Through mutual inductance M, a magnetic field created by an external current I_{ext} is applied and generates clockwise and counterclockwise currents. Because of the quantization of the enclosed flux ϕ, flux quantum Φ_0 can tunnel through the Josephson junction and the currents become the quantized states which are the basis for the flux qubit. Illustration taken from [13].

The flux qubit is made of three Josephson junctions all in the flux regime with a superconducting loop. When a magnetic field is applied through it, a clockwise or counterclockwise supercurrent is induced to decrease or increase the enclosed flux. These circulating supercurrents can form the basis states for the qubit. Regarding the decoherence properties, flux qubits are mostly sensitive to flux noise and fluctuations of the critical current as can be intuitively thought.

3) The phase qubit

It is studied and improved in the universities of Santa Barbara (UCSB) [15], Maryland and at the National Institute of Standards and Technologies (NIST) [16]. It is characterized by:

- $E_J \approx 10^4 E_C$

- size: $10 - 100 \mu m^2$

- Energy-level difference between the two lowest states: 10 GHz

- Coherence time: $T_2 = 0.1 - 1 \mu s$ (this can actually be improved by the design of the dielectrics)

The principle of the phase qubit is a Josephson junction biased by a large current. This bias induces a tilt in the potential of the Josephson junction (tilted-washboard potential). This reduces the number of bound states in the potential-energy well. Phase qubits manage to avoid the sensitivity to charge noise in increasing a little the critical-current noise.

4) The transmon qubit

It has been recently developed by the group in Yale [17] and the values given here are just referential. It is characterized by:

- $E_J \approx 10^2 E_C$

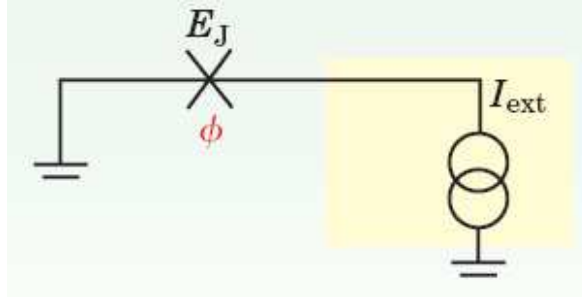- Energy-level difference between the two lowest states: 10 GHz

Figure 1.3: The phase qubit. The Josephson junction is driven by a current bias. This reduces the number of quantized states in the energy-potential and leads thus to a two-level-system. Illustration taken from [13].
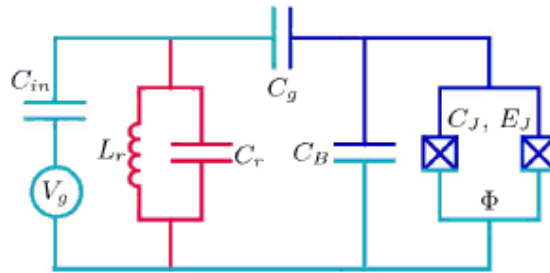

Figure 1.4: The transmon qubit. The circuit is very similar to the charge qubit. The states of the CPB will be those for the qubit and Cooper pairs can tunnel through a Josephson junction. However to reduce the sensitivity to the charge noise, a capacitance C_B is added to reduce the charge dispersion responsible for this noise. Illustration taken from [17].

- Coherence time (predicted): $T_2 \approx 35\mu s$

The design of the transmon qubit is closely related to the Cooper pair box of the charge qubit but there is an additional shunting connection of the two superconductors via a large capacitance C_B which which reduces the charging energy E_C. The main features of this new qubit is that the charge dispersion which determines the sensitivity of the Cooper pair box to charge noise reduces exponentially in E_J/E_C whereas the anharmonicity has an algebraic decay with a slow power law in E_J/E_C. So they manage to keep the advantage of the charge qubit, while increasing the average decoherence time T_2 drastically.

1.1.2 The one-dimensional microwave resonator

The resonator plays the role of the cavity. Two capacitances C_{in} and C_{out} at both ends of the centre narrow conductor play the role of the mirrors of an optical cavity. The field is sent inside the resonator through one of them and then stays in the resonator. The centre conductor and the ground planes at each side are usually made by patterning a thin superconducting film deposited on a silicon chip. The resonator behaves as a harmonic oscillator and can be modelled by a capacitor C and an inductance L in parallel near its resonance frequency which is thus $\omega_r = 1/\sqrt{LC}$. The resonator can contain one or more qubits. Their placement

depends on how many qubits we want to put inside and on which kind of resonator is used.
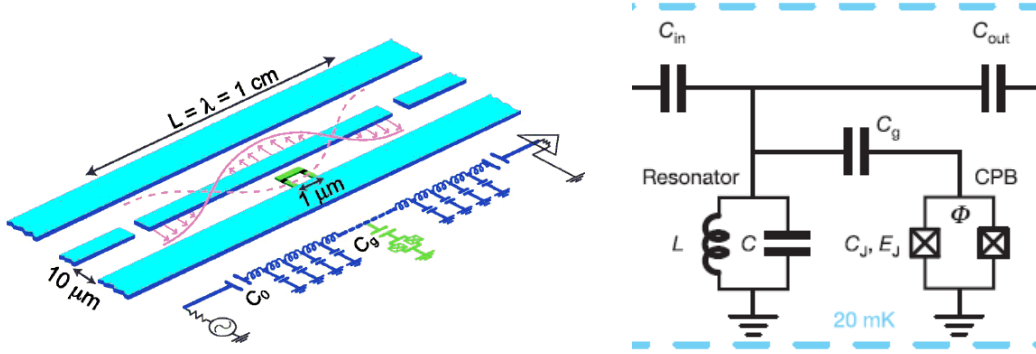

Figure 1.5: Left: Resonator with one SCqubit at the centre. The qubit is coupled to the resonator via a capacitance C_g. Two other capacitances C_{in} and C_{out} are placed at the end of the resonator. They play the role of the mirrors of an optical cavity. The resonator can be modeled by a capacitance C and inductance L near its resonance frequency. Right: Corresponding microwave circuit. Illustrations taken from [12] and [3] respectively.

This circuit behaves as a harmonic oscillator described by the Hamiltonian:

$$H_r = \hbar\omega_r(a^\dagger a + 1/2), \tag{1.1}$$

where $\langle a^\dagger a \rangle = n$ is the average photon number. The loss of photons of the resonator is due to the ports C_{in} and C_{out}, by which it is connected to the input and output transmission lines. The rate of dissipation is $\kappa = \omega_r/Q$ where Q is the quality factor of the resonator. Experimentally, the Yale group has $n < 0.06$ photon in the microwave resonator at a temperature $T < 100$ mK, and typical resonance frequencies are between 2 and 10 GHz.
Let us notice that in order to implement one or two-qubit gates, they have to send external driving fields on the resonator to drive the qubit inside it. The group of Yale, which has performed several experiments and proposals to implement gates, send these driving fields through the axis of the cavity according to Fig.1.5. Because of the high-quality factor Q of the resonator, the external fields are detuned from the resonator frequency. As a consequence, a lot of photons are reflected and the intensity of the driving fields has to be large to compensate this loss.

1.1.3 The two-dimensional cavity grid

This one-dimensional resonator is widely used cavity in Circuit QED experiments. However there are new proposed complex architectures which use this resonator as elementary building blocks. One of this proposition is the two-dimensional cavity grid [18]. We present here its main features and how it is possible to tune on resonance a chosen qubit with an external field or with a mode of the cavity.

The cavity array is formed of N horizontal and N vertical one-dimensional resonators. Each SCqubit is situated at the crossing point between two cavities. The external fields are sent in the axis of the resonator, far detuned from its frequency but they can be tuned on resonance with the transition frequency of the desired qubit. This allows the possibility to

realize logical operations in the resonant regime. As we will see this specific regime enables a fast realization of gates compared to the off-resonant regime.

From a technical point of view, to tune on resonance a SCqubit with the resonator field or with an external field, one has to change its transition frequency to the frequency of the desired field. It can be done with an external controlled current loop producing an additional magnetic field. This field will change the flux Φ of the qubit which is related with the Josephson coupling energy E_J. Using the fact that in SCqubits the level-spacing depends on this Josephson coupling energy, it is possible to control exactly the transition frequency of the qubit and thus to tune it on or off resonance with a field when we wish. Moreover this architecture allow to control each qubit independently or for instance all qubits in the same cavity at the same time.
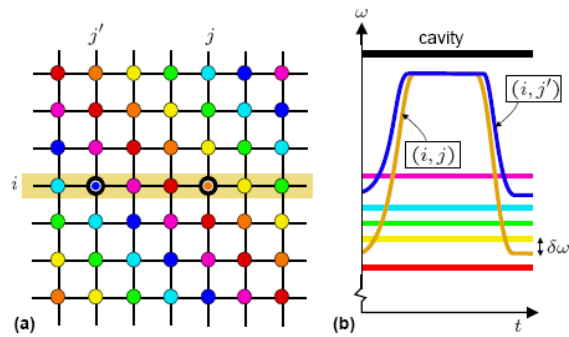

Figure 1.6: a) Architecture of a 2D cavity grid. Each line represents a one-dimensional resonator presented before and qubits which are denoted with circles are situated at the crossing point of two cavities. In a given cavity each qubit has a different transition frequency which can be changed by changing the parameters of the qubit. b) Two qubits can be tuned into mutual resonance by changing their transition frequencies. Illustration taken from [18].

Summary

In this section we presented the main devices of Circuit QED. In the next chapter we will focus on the realization of gates in the resonant regime and on the realization of multiqubit entangled states in Circuit QED. We will see that the implementation of resonant one- and two-qubit gates relies on the use of circuit cavity QED like the one-dimensional resonator presented here. Later when we will discuss the applications of these fast operations and we will work in the two-dimensional cavity grid and take advantage of this new architecture, especially for getting cluster states.

1.2 The qubit-resonator interaction

We will derive in this part the Hamiltonian which describes the interaction between a charge qubit and a resonator [12]. We choose this particular SCqubit for simplicity and because it was one of the first SCqubit developed. . However all kinds of SCqubits can be described as quantized two-level systems as exposed above and thus lead to the Jaynes-Cummings Hamil-

tonian too.

First we will show that the Hamiltonian describing the charge qubit without any interaction with another system is equivalent to that of a pseudo spin 1/2. If we suppose that the temperature is small enough, $T \ll T_C$, and that the voltage source is smaller than the gap of the Josephson junction, $|V| < \left|\frac{2\Delta}{e}\right|$, neither the thermal energy nor the external voltage source V are sufficient to break up Cooper pairs. Only the Cooper pairs are still able to tunnel through the junction (there is no more normal current nor a displacement current) and the only relevant degree of freedom is the number N of Cooper pairs on the island.

The Hamiltonian which describes this situation is:

$$H = 4E_C(N - N_g)^2 - E_J \cos\phi, \tag{1.2}$$

where

- $E_C = \frac{e^2}{2C_\Sigma}$ is the charging energy where $C_\Sigma = C_J + C_g$ is the total capacitance of the island,

- E_J is the coupling energy or Josephson energy,

- N is the charge operator which corresponds to the number of Cooper pairs on the island,

- $N_g = \frac{C_g V_g}{2e}$ is the dc gate charge (see Fig. 1.1 for the definition of C_g and the dc gate voltage V_g),

- ϕ is the phase-difference operator of the Josephson junction.

If we write the Hamiltonian in the eigenbasis of the charge operator N, we get:

$$H_Q = 4E_C \sum_N (N - N_g)^2 |N\rangle\langle N| - \frac{E_J}{2} \sum_N (|N+1\rangle\langle N| + \text{H.}c). \tag{1.3}$$

The first term desribes the charging energy of the Cooper pair box which is necessary to put one Cooper pair on the island. It can be derived from the classical laws of electrostatics. The second term corresponds to one Cooper pair tunneling through the Josephson junction.

We now go into the interaction picture to concentrate on the evolution due to the interaction of the different parts of the system. For this we apply the unitary operation to our Hamiltonian $U(t) = e^{-\frac{i}{\hbar}H_{\text{free}}t}$ where $H_{\text{free}} = 4E_C \sum_N (N - N_g)^2 |N\rangle\langle N|$. We obtain:

$$H_{\text{Qint}} = \frac{E_J}{2} \sum_N \left(e^{\frac{i}{\hbar}4E_C[2(N_g-N)-1]t}|N\rangle\langle N+1| + e^{-\frac{i}{\hbar}4E_C[2(N_g-N)-1]t}|N+1\rangle\langle N| \right). \tag{1.4}$$

All steps until now are valid for all kinds of SCqubits. Now we will have to consider the assumption of being in the charge regime where $E_C \gg E_J$. Indeed under this assumption, the tunneling perturbation is only effective between charge states that are almost resonant with each other. An alternative interpretation is that all the states off resonance with each other will be fast rotating terms and can be neglected in the rotating wave approximation. These almost resonant states appear at the degeneracy point $N_g = 1/2$ and are $|0\rangle$ and $|1\rangle$.

They will be the only relevant states in the Hamiltonian. If we go back into the Schrödinger picture, we get for the Hamiltonian:

$$H = 4E_C \sum_{N=0,1} (N - N_g)^2 |N\rangle\langle N| - \frac{E_J}{2}(|1\rangle\langle 0| + |0\rangle\langle 1|) \tag{1.5}$$

$$= -2E_C(1 - 2N_g)\sigma_z - \frac{E_J}{2}\sigma_x, \tag{1.6}$$

where $\sigma_z = |0\rangle\langle 0| - |1\rangle\langle 1|$ and $\sigma_x = |1\rangle\langle 0| + |0\rangle\langle 1|$.

This shows that the Cooper Pair Box is equivalent to a pseudo spin-1/2 particle with effective fields in the z and x directions.

Now we will consider the interaction of the Cooper pair box with the resonator which behaves as a harmonic oscillator to obtain the full dynamics [12]. It has been shown that this interaction arises due to an additional term in the gate voltage. It is now composed of the previously dc part and a new quantum part due to the quantized micowave field in the resonator:

$$V_g = V_g^{dc} + \sqrt{\frac{\hbar\omega_r}{Lc}} V(a + a^\dagger), \tag{1.7}$$

where a and $a^\dagger$ are the operators of annihilation and creation for a quantum of the resonator field. In consequence the gate charge will have an additional term

$$N_g = N_g^{dc} + \sqrt{\frac{\hbar\omega_r}{Lc}}(a + a^\dagger). \tag{1.8}$$

We insert this full expression in the Hamiltonian and we obtain the interaction between the Cooper pair box and the resonator. One of the terms corresponds to a renormalization of the resonator frequency and another can be neglected when considering the rotating wave approximation. The Hamiltonian after these two approximations is:

$$H_{\mathrm{QR}} = -2E_C(1 - 2N_g^{dc})\sigma_z - \frac{E_J}{2}\sigma_x - e\frac{C_g}{C_\Sigma}\sqrt{\frac{\hbar\omega_r}{Lc}}(a + a^\dagger) \times (1 - 2N_g - \sigma_z). \tag{1.9}$$

We have disregarded the term $(2a^\dagger a + 1)$ corresponding to the renormalization of the cavity frequency, and we have neglected the term $((a^\dagger)^2 + a^2)$ considering the rotating wave approximation.

If we take into account the energy of the resonator, we finally get the Hamiltonian of Circuit QED with a Cooper pair box:

$$H_{\mathrm{cQED}} = \hbar\omega_r a^\dagger a - 2E_C(1 - 2N_g^{dc})\sigma_z - \frac{E_J}{2}\sigma_x - e\frac{C_g}{C_\Sigma}\sqrt{\frac{\hbar\omega_r}{Lc}}(a + a^\dagger) \times (1 - 2N_g - \sigma_z). \tag{1.10}$$

We now want to make the analogy between the Hamiltonians of Circuit QED and of the Jaynes-Cummings model. For this we look for the eigenvectors of the Hamiltonian of the SCqubit

$$H_Q = -2E_C(1 - 2N_g^{dc})\sigma_z - \frac{E_J}{2}\sigma_x, \tag{1.11}$$

which are:

$$
\begin{align}
|\uparrow\rangle &= \cos(\theta/2)|1\rangle + \sin(\theta/2)|0\rangle \tag{1.12}\\
|\downarrow\rangle &= -\sin(\theta/2)|1\rangle + \cos(\theta/2)|0\rangle, \tag{1.13}
\end{align}
$$

where $\theta = \arctan\left[\frac{E_J}{4E_C(1-2N_g^{dc})}\right]$ is the mixing angle.

Expressing the Circuit QED Hamiltonian in this new basis ($\sigma_z = |\uparrow\rangle\langle\uparrow| - |\downarrow\rangle\langle\downarrow|$), it leads to:

$$
\begin{align}
H &= \hbar\omega_r a^\dagger a + \frac{\hbar\omega_a}{2}\sigma_z - e\frac{C_g}{C_\Sigma}\sqrt{\frac{\hbar\omega_r}{Lc}}(a+a^\dagger) \times (1 - 2N_g - \cos\theta\sigma_z + \sin\theta\sigma_x)\\
&= \hbar\omega_r a^\dagger a + \frac{\hbar\omega_a}{2}\sigma_z - \hbar g(a+a^\dagger) \times (1 - 2N_g - \cos\theta\sigma_z + \sin\theta\sigma_x), \tag{1.14}
\end{align}
$$

where

- $g = \frac{eC_g}{\hbar C_\Sigma}\sqrt{\frac{\hbar\omega_r}{cL}}$ is the coupling constant,

- $\omega_a = \frac{\sqrt{E_J^2 + \left(4E_C(1-2N_g^{dc})\right)^2}}{\hbar}$ is the splitting energy of the qubit.

We now go again into the interaction picture to see which terms are really relevant during the interaction. This time, the unitary operation we have to apply takes the form:

$$
U(t) = e^{-i(\omega_r a^\dagger a + \frac{\omega_a}{2}\sigma_z)t}. \tag{1.15}
$$

We obtain:

$$
H_{\text{int}} = \hbar g\left(ae^{-i\omega_r t} + a^\dagger e^{i\omega_r t}\right)\left(1 - 2N_g - \cos\theta\sigma_z + \sin\theta(\sigma_+ e^{i\omega_a t} + \sigma_- e^{-i\omega_a t})\right). \tag{1.16}
$$

If we suppose that the cavity frequency is close to the transition frequency of the SCqubit, we can neglect the fast oscillating terms which is the rotating wave approximation (RWA). This yields finally the interaction Hamiltonian:

$$
H_{\text{int}} = \hbar g\sin\theta\left(a\sigma_+ e^{-i(\omega_r-\omega_a)t} + a^\dagger\sigma_- e^{+i(\omega_r-\omega_a)t}\right). \tag{1.17}
$$

To bring to light the analogy with the Jaynes-Cummings model, we go back to the Schrödinger picture and get:

$$
H_{JC} = \hbar\omega_r a^\dagger a + \frac{\hbar\omega_a}{2}\sigma_z + \hbar g\sin\theta(a\sigma_+ + a^\dagger\sigma_-). \tag{1.18}
$$

This corresponds exactly to the Jaynes-Cummings Hamiltonian with a coupling constant $g\sin\theta$. In the optimal case of $\theta = \pi/2$, this coupling is maximal. The point where this case occurs is called the degeneracy point, where $N_g = 1/2$, $\theta = \pi/2$ and $\omega_0 = E_J/2$.
Nevertheless the particularity of this demonstration is that we did not use the hypothesis of being at this degeneracy point. This shows that the analogy with Jaynes-Cummings is still valid even if we do not consider the SCqubit at this particular point. This will be useful in the following because it will not be always possible to stay at the degeneracy point for the purposes of this work.

Summary

We motivated the field of Circuit QED and showed that it corresponds to the realization of Cavity QED in solid-state systems, the full dynamics being described by the Jaynes-Cummings model. Then we presented the principal devices which are studied at the moment, with their characteristics. We have now the fundamental knowledge to go into the field of standard quantum computation.

In the next chapter we will study the basic tools to implement quantum circuits and maybe quantum algorithms. These tools are the universal one- and two-qubit gates which allow to build any circuit in combining them. Because we saw that the decoherence of all qubits is a major problem even if improvements have been made, the aim of all the work will be to implement all the operations in a faster way.

Fast operations mean that they are performed in the resonant regime to be compared to the off-resonant or dispersive regime which will be explained later. As we will see, lots of gates are still realized in the dispersive regime where they are slow. The next chapter will thus constitute a possible improvement in the speed of the experimental realizations of gates and circuits.

Chapter 2

Toolbox of resonant operations

Quantum circuits are composed of wires transmitting the information and quantum gates manipulating the state of quantum physical systems, the qubits. In order to build a quantum circuit useful for implementing algorithms or error correction codes, there exist different set of gates which form the "universal gates". They permit the construction of any operation between an arbitrary number of qubits. The universal gates are composed of two main types of operations: the one-qubit gates performing local operations and the two-qubit gates which operate on two qubits. We will present four one-qubit gates, the rotations around the three axis of the Bloch sphere with an arbitrary angle and the Hadamard gate, and three two-qubit gates, the CPHASE, the iSWAP and the $\sqrt{\text{iSWAP}}$. The goal will be to implement them in a fast way in Circuit QED in order to satisfy the constraint of decoherence of the SCqubits as mentioned before. It constitutes one of the crucial conditions for implementing useful quantum computing schemes.

First of all we have to explain what is a fast operation and to what it can be compared. In quantum information an operation can be implemented by using the interaction between a two-level system and either an external driving field or modes of the cavity field. The interaction corresponds to an exchange of energy between the two systems and is characterized by the Rabi frequency. By convention it is usually denoted Ω_R in the case of an external driving field and g in the case of a mode of the cavity field. This coupling constant corresponds to the time needed for the two-level system to undergo a full Rabi oscillation between its ground level and excited level. More generally the speed of an operation is given by the effective coupling constant in the interaction Hamiltonian.

Two main regimes are important for the further work: the resonant regime and the off-resonant regime. They can be distinguished by comparing the Rabi frequency to Δ, where Δ is the detuning between the transition frequency of the two-level system and the frequency of the field. The resonant regime occurs when $\Delta = 0$ and in this particular case, the coupling strength is Ω_R. The off-resonant regime is reached when $\Omega_R \ll \Delta$ and the corresponding coupling rate is $\frac{\Omega_R^2}{\Delta}$. When we compare these two rates, the condition of large detuning implies that $\frac{\Omega_R^2}{\Delta} \ll \Omega_R$ in any case and as a consequence, an operation in the off-resonant regime is always slower than an operation in the resonant regime.

In the next section we will concentrate on the realization of the universal one-qubit gates which are the rotations around the $\hat{x}$, $\hat{y}$, and $\hat{z}$ axis of the Bloch sphere and the Hadamard gate, which can be obtained by combining these three rotations. As we will see, the rotations

around the $\hat{x}$ and $\hat{y}$ axis are naturally performed in the resonant regime by sending an external field on the qubit with a different phase for each rotation. Concerning the z rotation, it is more delicate. Indeed the effect of this rotation on a state is to add a phase to this state in addition to the free evolution. There are two ways to do it. As a first possibility we can change the transition frequency of the qubit in a controlled way which will lead directly to the desired z rotation. This corresponds to a dc-Stark shift and it is a very fast operation. Let us notice that experimentally it is possible to change the transition frequency of the qubit in a very precise way as explained in chapter 1 when we have to tune on resonance a qubit with the frequency of one cavity of the two-dimensional cavity grid. There is an alternative possibility if we do not want to play with the qubit-transition frequency to implement operations. As for the x and y rotations, we can send an external field on the qubit to drive it. However in this case we need to go in the off-resonant regime to get the σ_z Pauli matrix. This corresponds to an ac-Stark shift and implies that in this case the z rotation is much slower than the x and y rotations.

In this work we will suppose that we will change the transition frequency of the qubit only to put it in resonance with the desired systems or transitions we want but not to implement operations. Therefore we will consider the z rotation as an ac-Stark shift and we will see if it is possible to avoid the use of the ac-Stark shift in other universal operations such as the Hadamard gate.

2.1   Universal one-qubit operations

2.1.1   Rotations in the Bloch sphere around the $\hat{x}$, $\hat{y}$ and $\hat{z}$ axis
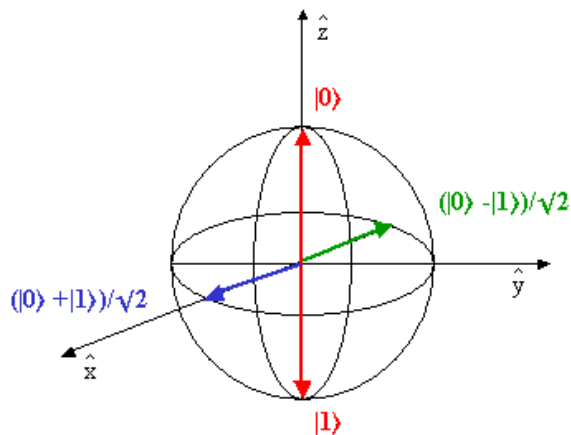
Figure 2.1: The Bloch sphere. Representation of the states $|0\rangle$, $|1\rangle$ and superposition state $(|0\rangle + |1\rangle)/\sqrt{2}$.

We will expose now in more detail the three rotations and derive the interaction Hamiltonian that leads to the correct rotation. We will use the general language of quantum optics to describe the operations but this is rigorously valid for Circuit QED because the Hamiltonian of Circuit QED follows the Jaynes-Cummings model. For instance, the two-level system can

correspond to one of the SCqubits presented before and the cavity can be the one-dimensional microwave resonator.

The σ_x-rotation and its evolution operator

The physical system is composed of a quantized two-level system driven by a classical field. We will present now the Hamiltonians describing these elements and then derive the interaction Hamiltonian [19, 20]. This will lead to the σ_x Pauli matrix and thus to the rotation around the $\hat{x}$ axis in the Bloch sphere.
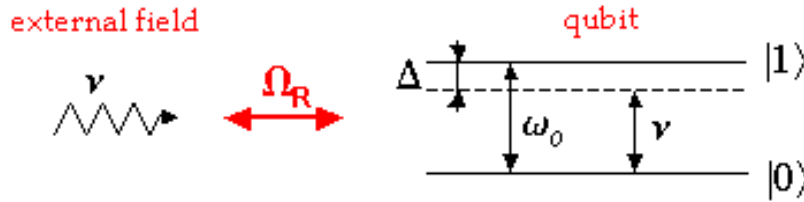

Figure 2.2: Physical system. An external field with frequency ν is sent to the qubit which transition frequency is ω_0. The detuning between both frequencies is denoted Δ. The Rabi frequency or coupling strength is Ω_R.

We will describe the two-level system in its eigenbasis $\{|a\rangle, |b\rangle\}$. The Hamiltonian can be written as:

$$H_0 = \hbar\omega_a|a\rangle\langle a| + \hbar\omega_b|b\rangle\langle b|. \tag{2.1}$$

We shift the energies by the average of the energies of the system, $\frac{1}{2}\hbar(\omega_a + \omega_b)$. We can now write the unperturbed Hamiltonian as:

$$H_0 = \frac{\hbar\omega_0}{2}\sigma_z, \tag{2.2}$$

where $\omega_0 = \omega_a - \omega_b$.

We suppose that the classical driving field is a monochromatic planar wave field polarized along the $\hat{x}$ axis. Let us notice that in Circuit QED the polarization is fixed by the resonator geometry. The expression of the field is:

$$\overrightarrow{E}(t) = \left(E_0 e^{-i(\nu t+\phi)} + E_0^* e^{i(\nu t+\phi)}\right) \cdot \hat{x}, \tag{2.3}$$

where

- E_0 is the complex amplitude of the field,

- ν is the frequency of our electric field,

- ϕ is an arbitrary phase.

To obtain the corresponding interaction Hamiltonian, we will follow the further steps. We will first consider the dipolar approximation, then we will go into the interaction picture and we will finally apply the rotating wave approximation.

The dipolar approximation is valid when $\overrightarrow{k} \cdot \overrightarrow{r} \ll 1$ where $\overrightarrow{k} = (k_x, k_y, k_y)$ is the wave vector of the field and $\overrightarrow{r}$ is the distance between the two charges of the dipole. This means

that the wavelength of the field must be larger than the characteristic size of the atomic system. In the case of Circuit QED the wavelength is of the order of millimeter while the artificial atom's size is around micrometer. The condition is thus satisfied.

The general expression of the interaction Hamiltonian in this approximation takes the usual form:

$$H_{dip} = -\overrightarrow{d} \cdot \overrightarrow{E}(\overrightarrow{r}, t), \tag{2.4}$$

where $\overrightarrow{d}$ is the dipole moment of the artificial atom. We want to express this interaction in the eigenbasis of the two-level atom. Using the closure relation $|a\rangle\langle a| + |b\rangle\langle b| = 1$, we get:

$$
\begin{aligned}
H_{dip} &= -\big(|a\rangle\langle a| + |b\rangle\langle b|\big) d_x \big(|a\rangle\langle a| + |b\rangle\langle b|\big) E(t) \\
&= -(\rho_{ab}|a\rangle\langle b|) + \rho_{ba}|b\rangle\langle a|) E(t) \\
&= -(\rho_{ab}\sigma_+ + \rho_{ba}\sigma_-) E(t),
\end{aligned} \tag{2.5}
$$

where $\rho_{ab} = \rho_{ba}^* = \langle a|d_x|b\rangle$ is the matrix element of the electric dipole moment and d_x is the x component of the dipole.

Using the Euler decomposition $\rho_{ab} = |\rho_{ab}|e^{i\phi_{ab}}$ and $E_0 = |E_0|e^{i\phi_{E_0}}$, we redefine the operators to take into account the additional phase. We are so able to factorize the global expression taking into account the expression of the classical field. We get:

$$
\begin{aligned}
H_{dip} &= -(\rho_{ab}\sigma_+ + \rho_{ba}\sigma_-)(E_0 e^{-i(\nu t+\phi)} + E_0^* e^{i(\nu t+\phi)}) \\
&= -\Omega_R \hbar (\sigma_+ + \sigma_-)(e^{-i(\nu t+\phi)} + e^{i(\nu t+\phi)}),
\end{aligned} \tag{2.6}
$$

where $\Omega_R = \frac{|\rho_{ab}||E_0|}{\hbar}$ is the classical Rabi frequency that characterizes the exchange of energy between the two-level system and one mode of the field. Therefore it depends only on parameters of these systems, ρ_{ab} and the amplitude of the field E_0 and on the Planck constant $\hbar$.

We now go into the interaction picture to concentrate strictly on the evolution due to the interacting systems. We do not care about the free evolution anymore. We apply the evolution unitary operator $U(t) = e^{-iH_0 t/\hbar}$ where $H_0 = \frac{\hbar\omega_0}{2}\sigma_z$ on the Hamiltonian $H_I(t) = U^\dagger(t)H_{dip}U(t)$. We obtain the interaction Hamiltonian in the interaction picture:

$$H_I(t) = -\hbar\Omega_R(\sigma_+ e^{i\omega_0 t} + \sigma_- e^{-i\omega_0 t})(e^{-i(\nu t+\phi)} + e^{i(\nu t+\phi)}), \tag{2.7}$$

where we have used the relations:

- $\sigma_z = 2\sigma_+\sigma_- - 1$

- $e^{i\frac{\omega_0}{2}\sigma_z t}\sigma_+ e^{-i\frac{\omega_0}{2}\sigma_z t} = e^{i\omega_0\sigma_+\sigma_- t}\sigma_+ e^{-i\omega_0\sigma_+\sigma_- t} = \sigma_+ e^{i\omega_0 t}$

- $e^{i\frac{\omega_0}{2}\sigma_z t}\sigma_- e^{-i\frac{\omega_0}{2}\sigma_z t} = e^{i\omega_0\sigma_+\sigma_- t}\sigma_- e^{-i\omega_0\sigma_+\sigma_- t} = \sigma_- e^{-i\omega_0 t}$

The additional phase ϕ is important because the x and y rotations differ by a phase-factor of $\pi/2$. For the x rotation, we set $\phi = \pi$ to simplify the expression 2.7 and this will be the reference for the y rotation in the next section. We get:

$$
\begin{aligned}
H_I(t) &= \hbar\Omega_R(\sigma_+ e^{i\omega_0 t} + \sigma_- e^{-i\omega_0 t})(e^{-i\nu t} + e^{i\nu t}) \\
&= \hbar\Omega_R(\sigma_+ e^{i(\omega_0-\nu)t} + \sigma_+ e^{i(\omega_0+\nu)t} + \sigma_- e^{-i(\omega_0+\nu)t} + \sigma_- e^{-i(\omega_0-\nu)t}). \quad (2.8)
\end{aligned}
$$

We consider that we send the field with a frequency near the transition frequency of the two-level system such that the fast oscillating terms of the form $e^{\pm i(\omega_0+\nu)t}$ can be neglected. This is the rotating wave approximation (RWA) and we obtain:

$$
H_I(t) = \hbar\Omega_R(\sigma_+ e^{i(\omega_0-\nu)t} + \sigma_- e^{-i(\omega_0-\nu)t}). \quad (2.9)
$$

A particular case is the resonant regime for which $\omega_0 = \nu$:

$$
H_{\sigma_x} = \hbar\Omega_R(\sigma_+ + \sigma_-) = \hbar\Omega_R\sigma_x. \quad (2.10)
$$

We observe that we obtain exactly the Hamiltonian corresponding to a x rotation in the Bloch sphere.
The corresponding evolution operator is defined as:

$$
U(t) = e^{-iH_{\sigma_x}t/\hbar} = e^{-i\Omega_R\sigma_x t}. \quad (2.11)
$$

To get the known expression of $R_x(\theta)$ [21], we use the Taylor expansion for the exponential and the following relations:

- $\sigma_x^{2k} = 1, k = 0, 1, 2, ...$

- $\sigma_x^{2k+1} = \sigma_x, k = 0, 1, 2, ...$

- $(-i)^{2k} = (-1)^k, k = 0, 1, 2, ...$

- $(-i)^{2k+1} = -i(-1)^k, k = 0, 1, 2, ...$

We get:

$$
e^{-i\Omega_R\sigma_x t} = \sum_{k=0}^{\infty} \frac{(-i\sigma_x\Omega_R t)^k}{k!} = \cos(\Omega_R t)\mathbb{I} - i\sigma_x \sin(\Omega_R t). \quad (2.12)
$$

$$
U_{\sigma_x} = \begin{pmatrix} \cos(\Omega_R t) & -i\sin(\Omega_R t) \\ -i\sin(\Omega_R t) & \cos(\Omega_R t) \end{pmatrix}.
$$

It is usually written as:

$$
R_x(\theta) = \begin{pmatrix} \cos(\theta/2) & -i\sin(\theta/2) \\ -i\sin(\theta/2) & \cos(\theta/2) \end{pmatrix},
$$

where the rotation angle $\theta = 2\Omega_R t$ can be set by choosing specific values for the time during which the microwave pulse is switched on and for the Rabi frequency which depends on the amplitude E_0 of the external classical driving field.

The σ_y-rotation and its evolution operator

The rotation around the $\hat{y}$ axis in the Bloch sphere corresponds to the x rotation with a phase-difference of $\pi/2$. So, compared to the phase reference ϕ, we chose $\phi = \pi/2$ in Eq.(2.7) and it leads to the following interaction Hamiltonian:

$$H_{\sigma_y} = \hbar\Omega_R(i\sigma_- - i\sigma_+) = \hbar\Omega_R\sigma_y. \tag{2.13}$$

Again the corresponding evolution operator is given by:

$$U(t) = e^{-i\Omega_R\sigma_y t}, \tag{2.14}$$

which can be written in the form of:

$$U_{\sigma_y} = \cos(\Omega_R t)\mathbb{I} - i\sigma_y\sin(\Omega_R t). \tag{2.15}$$

$$U_{\sigma_y} = \begin{pmatrix} \cos(\Omega_R t) & -\sin(\Omega_R t) \\ \sin(\Omega_R t) & \cos(\Omega_R t) \end{pmatrix},$$

equivalent to the usual expression:

$$R_y(\theta) = \begin{pmatrix} \cos(\theta/2) & -\sin(\theta/2) \\ \sin(\theta/2) & \cos(\theta/2) \end{pmatrix}.$$

So sending an external field in resonance with the qubit allows to produce the x and y rotations. The axis depends on which additional phase we choose for the field.

The σ_z- rotation

As explained at the beginning of the section, we consider only the z rotation as an ac-Stark shift in this work. In this paragraph, we will try to give some intuitive idea concerning the off-resonant or dispersive regime and the speed of an operation in this particular regime.

When we send an external driving field, it is not possible to get the z-Pauli matrix in the interaction Hamiltonian directly by changing the phase for instance. It is necessary to go into the off-resonant regime which is reached when $\Delta \gg \Omega_R$. A large detuning means that the photons of the field will not have the correct energy to excite the atom directly. This corresponds to the first order process in the coupling strength Ω_R. At the second order the photon will leave a trace of its attempt to excite the atom. It corresponds to an ac-Stark shift (virtual excitation of the atom by the photon), and the corresponding rate is Ω_R^2/Δ. To go into the dispersive regime, we have to perform a unitary transformation up to the second order in Ω_R which eliminates the direct coupling of the first order. This leads to the following interaction Hamiltonian:

$$H_{\sigma_z} = \hbar\frac{\Omega_R^2}{\Delta}\sigma_z. \tag{2.16}$$

The corresponding evolution operator is:

$$\begin{aligned} U_{\sigma_z}(t) &= e^{-\frac{i}{\hbar}H_{\sigma_z}t} \\ &= \cos(\frac{\Omega_R^2}{\Delta}t)\mathbb{I} - i\sigma_z\sin(\frac{\Omega_R^2}{\Delta}t), \end{aligned} \tag{2.17}$$

which leads to:

$$U_{\sigma_z}(t) = \begin{pmatrix} e^{-i\frac{\Omega_R^2}{\Delta}t} & 0 \\ 0 & e^{i\frac{\Omega_R^2}{\Delta}t} \end{pmatrix}.$$

We find again the well-known expression for a rotation around the $\hat{z}$ axis:

$$R_z(\theta) = \begin{pmatrix} e^{-i\theta/2} & 0 \\ 0 & e^{i\theta/2} \end{pmatrix},$$

where $\theta/2 = \frac{\Omega_R^2}{\Delta}t$.

Summary

By sending an external classical driving field on a two-level atom, we know how to perform the rotations about the $\hat{x}$ and $\hat{y}$ axis in the Bloch sphere. They are naturally in the resonant regime and therefore faster. To perform the z rotation, we have to go in the dispersive regime where the speed of the operation is smaller due to the lower rate at which the coupling works. We have to avoid this kind of operations in quantum computation because this reduces the number of gates which can be implemented in the finite coherence time of SCqubits. In the next section, we will present the Hadamard gate and study how to realize it in a fast way.

2.1.2   The Hadamard gate

Current definition and experimental implementation

The Hadamard gate is an essential one-qubit gate because it is part of different sets of universal gates required to realize every two-qubit gate [21]. Its matrix form is:

$$H = \frac{1}{\sqrt{2}} \begin{pmatrix} 1 & 1 \\ 1 & -1 \end{pmatrix}.$$

In the Bloch sphere, this matrix corresponds to a rotation of an angle π around the axis defined by the vector $\hat{n} = \left(1/\sqrt{2}, 0, 1/\sqrt{2}\right)$ with a global phase $\phi = \pi/2$.

Usually the way to write the Hadamard gate is as a function of the rotations around the $\hat{x}$, $\hat{y}$ and $\hat{z}$ axis of the Bloch sphere [21]. The well-known expression is:

$$H = e^{i\pi/2} R_x(\frac{\pi}{2}) R_z(\frac{\pi}{2}) R_x(\frac{\pi}{2}), \tag{2.18}$$

where

$$R_x(\theta) = \begin{pmatrix} \cos(\theta/2) & -i\sin(\theta/2) \\ -i\sin(\theta/2) & \cos(\theta/2) \end{pmatrix}$$

and

$$R_z(\theta) = \begin{pmatrix} e^{-i\theta/2} & 0 \\ 0 & e^{i\theta/2} \end{pmatrix}.$$

This gate is characterized by:

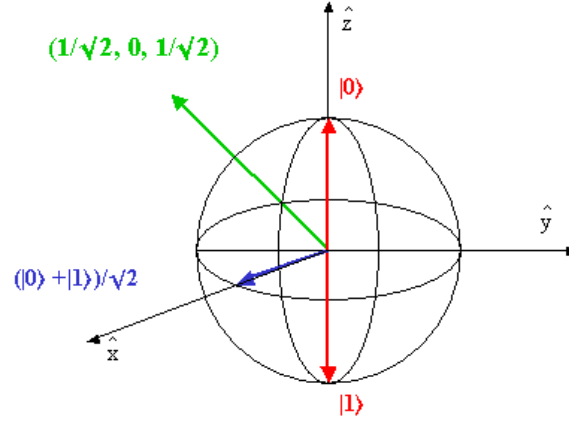- 3 pulses

- 2 changes in the frequency.

Figure 2.3: Representation of the Hadamard gate's effect on the states $|0\rangle$ and $|1\rangle$. The state $|0\rangle$ is put in the superposition state $(|0\rangle + |1\rangle)/\sqrt{2}$ shown in blue and the state $|1\rangle$ is put in the superposition state $(|0\rangle + |1\rangle)/\sqrt{2}$ shown in green.

The Yale group has already proposed a method to perform it [12]. With their experimental setup they can perform a rotation around any axis in the Bloch sphere and thus in particular around the axis defined by $\left(1/\sqrt{2}, 0, 1/\sqrt{2}\right)$ corresponding to the Hadamard gate for an angle π.
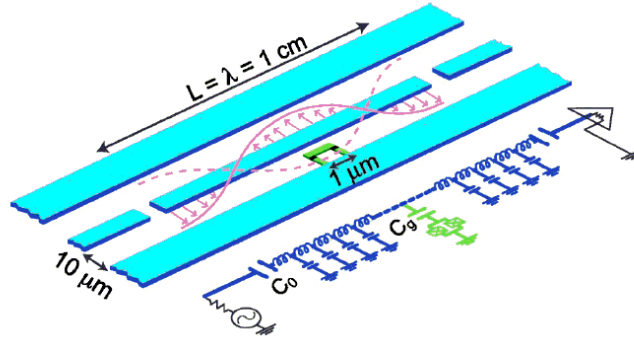
Figure 2.4: Experimental setup for Circuit QED from the group of Yale. Illustration taken from [12].

The physical system is composed of a charge qubit placed inside a one-dimensional resonator which is driven by an external field. The corresponding Hamiltonian in the rotating frame of the driving field is:

$$H = \Delta_r a^\dagger a + \frac{\Delta_a}{2}\sigma_z - g(a^\dagger \sigma_- + \sigma_+ a) + \frac{\Omega_R}{2}\sigma_x, \tag{2.19}$$

where

- $\Omega_R = \frac{2Eg}{\Delta_r}$ is the Rabi frequency,

- E is the amplitude of the driving field,

- $\Delta_r = \omega_r - \omega_d$ is the detuning between the resonator and the classical driving field (we work in a frame rotating at ω_d),

- $\Delta_a = \omega_a - \omega_d$ is the detuning between the SCqubit and the classical driving field,

- $\Delta = \omega_a - \omega_r$ is the detuning between the SCqubit and the resonator.

As explained in the first chapter, they send the driving field in the axis of the cavity far detuned from the resonator frequency. As a consequence they work in the off resonant regime: there is no direct coupling between the driving field and the qubit. Mathematically it is equivalent to apply a unitary transformation on the Hamiltonian to drop off this direct coupling. It yields the following expression:

$$\tilde{H} = \Delta_r a^\dagger a + \frac{\tilde{\Delta}_a}{2}\sigma_z + \frac{\Omega_R}{2}\sigma_x, \tag{2.20}$$

where $\tilde{\Delta}_a = \omega_a - \omega_d + \frac{g^2}{\Delta}$. They can thus implement rotations in the x-z plane playing with the parameters $\tilde{\Delta}_a$ and Ω_R.

Our improvement

One manner to increase the speed of the operations is to avoid the ac-Stark shift equivalent to the z rotation. Our enhancement will consist in demonstrating that the Hadamard gate can be realized with another combination of rotations in the Bloch sphere, in fact only around the $\hat{x}$ and $\hat{y}$ axis which are resonant operations.

We were inspired for the alternative expression of the Hadamard gate by the book "Quantum computation and Quantum information" [21]. The key point is that any rotation in the Bloch sphere which is a unitary operation can be decomposed using only the x and y rotations with four parameters according to the following expression:

$$U = e^{i\alpha} R_x(\beta) R_y(\gamma) R_x(\delta), \tag{2.21}$$

where α is a global phase and β, γ, δ are the angles of the different rotations.

As it has been derived in the last section, the matrix expressions of each rotation are:

$$R_x(\theta) = \begin{pmatrix} \cos(\theta/2) & -i\sin(\theta/2) \\ -i\sin(\theta/2) & \cos(\theta/2) \end{pmatrix},$$

$$R_y(\theta) = \begin{pmatrix} \cos(\theta/2) & -\sin(\theta/2) \\ \sin(\theta/2) & \cos(\theta/2) \end{pmatrix}.$$

We find for U:

$$U = e^{i\alpha} \times \begin{pmatrix} \cos\gamma/2\cos\chi_+ - i\sin\gamma/2\sin\chi_- & -\sin\gamma/2\cos\chi_- - i\cos\gamma/2\sin\chi_+ \\ \sin\gamma/2\cos\chi_- - i\cos\gamma/2\sin\chi_+ & \cos\gamma/2\cos\chi_+ + i\sin\gamma/2\sin\chi_- \end{pmatrix},$$

where $\chi_+ = (\beta/2 + \delta/2)$ and $\chi_- = (\beta/2 - \delta/2)$.

To ensure that this expression is indeed a unitary operation in the Bloch sphere, we checked that:

- $\det U = \pm 1$.

- $UU^\dagger = U^\dagger U = 1 \Leftrightarrow$ Rows and columns are orthonormals.

This enables us to write the z rotation as a function of the x and y rotations. The required values of parameters $\alpha, \beta, \gamma, \delta$ are:

$$
\begin{cases}
\alpha = 0 \\
\beta = \pi/2 \\
\gamma = \gamma \\
\delta = -\pi/2
\end{cases}
$$

The z rotation corresponds to:

$$R_z(\theta) = R_x(\pi/2)R_y(\theta)R_x(-\pi/2) \tag{2.22}$$

Finally, substituting Eq. (2.22) in the expression of the Hadamard gate Eq. (2.18), it gives:

$$
\begin{aligned}
H &= e^{i\pi/2}R_x(\pi/2)R_z(\pi/2)R_x(\pi/2) \\
&= e^{i\pi/2}R_x(\pi/2)R_x(\pi/2)R_y(\pi/2)R_x(-\pi/2)R_x(\pi/2) \\
&= e^{i\pi/2}R_x(\pi)R_y(\pi/2). \tag{2.23}
\end{aligned}
$$

This new expression has several advantages in comparison with the initial one (Eq. (2.18)). First only rotations around the $\hat{x}$ and $\hat{y}$ axis are used, which was the main goal. These operations are fast. Second it is composed of only two pulses instead of three. Finally experimentally, due to the fact that the y rotation can be obtained from the x one adding a $\pi/2$-phase, this expression will require one change in phase to pass from the x pulse to the y pulse. This can be done directly with a microwave generator. It has to be compared to two changes in the frequency to perform the x, z and x rotations.

Experimental realizations

To be more concrete and justify our claim that it is a new efficient way to realize the Hadamard gate, we propose in this section two possibilities to produce the required pulses for the fast Hadamard gate:

$$H = e^{i\pi/2}R_x(\pi)R_y(\pi/2). \tag{2.24}$$

One possibility to implement this operation is to send two pulses that have the same amplitude (the coupling which is the Rabi frequency will be the same) and we have thus to define two times so that:

- $\Omega_R t_1 = \frac{\pi}{2}$ corresponds to $R_x(\pi)$

- $\Omega_R t_2 = \frac{\pi}{4}$ corresponds to $R_y(\pi/2)$

Another possibility is to take two different amplitudes for the two subsequent pulses and to use the same time duration. Because the rotation around the $\hat{x}$ axis is defined by an angle twice the angle for the y rotation, the amplitude of the x pulse has to be the double of the amplitude of the y pulse:

- $\Omega_{R_1} t = \frac{\pi}{2}$ corresponds to $R_x(\pi)$

- $\Omega_{R_2} t = \frac{\pi}{4}$ corresponds to $R_y(\pi/2)$

where $\Omega_{R_1} = 2\Omega_{R_2}$.

We will now present two experimental setups which permit the realization of the Hadamard gate. The first setup is composed of two microwave generators. One produces the x pulse with the correct amplitude and time, then the second produces the y pulse. They are subsequently sent to the qubit. This is schematized in Fig. 2.5.
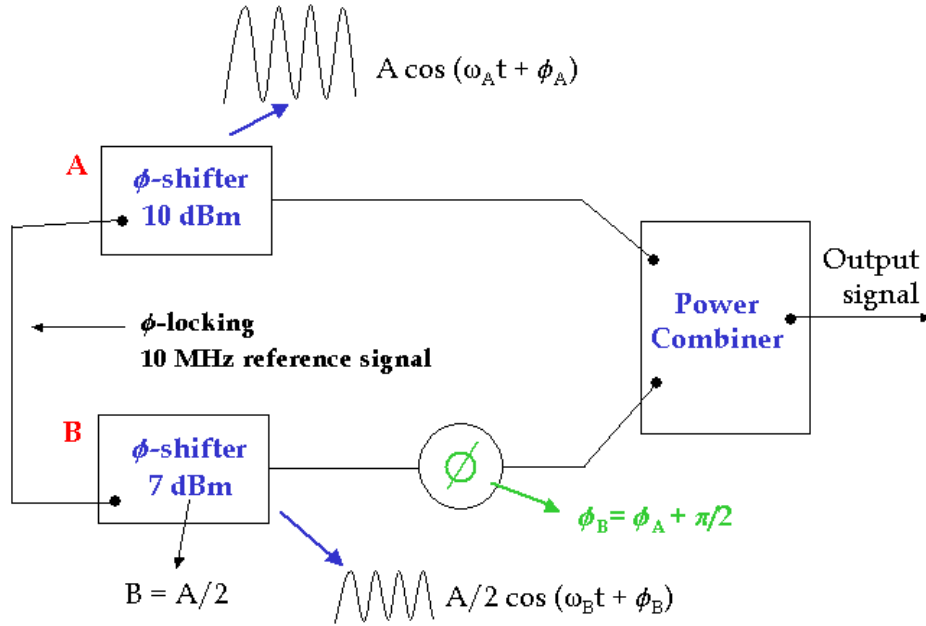

Figure 2.5: Experimental setup for the generation of the pulses required for the fast Hadamard gate using two microwave generators A and B. B produces a pulse with an amplitude half the one of A. In order to produce the y rotation, a phase-shifter adds a phase $\pi/2$ to the sinusoidal B compared to the sinusoidal A. Finally, the two pulses arrive in a power combiner which sends them one after the other to the qubit.

The second setup is an improved one. Instead of using two microwave generators, it uses an I/Q mixer which is an electronic device allowing the generation of the two pulses with only one microwave generator The scheme is shown in Fig. 2.6.

Summary

We proved an alternative expression for the Hadamard gate using only the resonant operations corresponding to rotations around the $\hat{x}$ and $\hat{y}$ axis. We showed that it has several advantages such as a smaller number of pulses and only resonant operations. We then briefly exposed how to realize it experimentally.

A next step in getting all the tools for quantum computing is to deal with two-qubit operations. This is the subject of the next section.
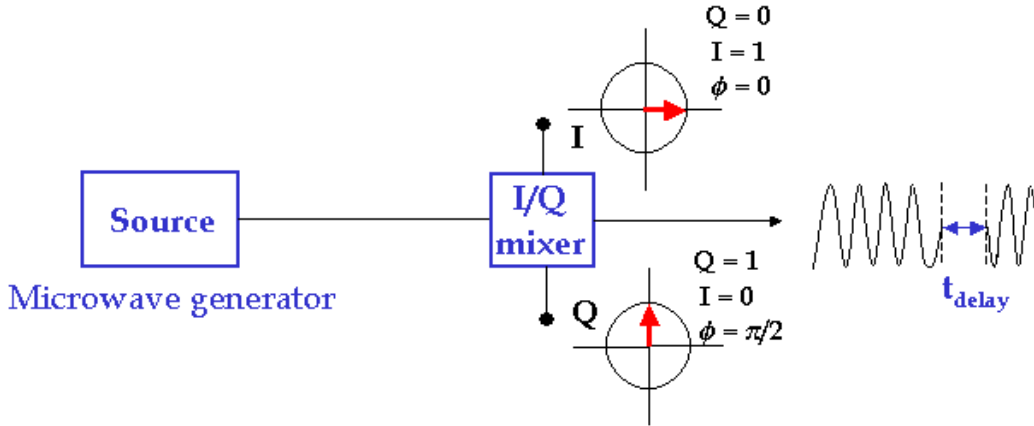
Figure 2.6: Experimental setup for the generation of two subsequent pulses with one microwave generator via an I/Q mixer (In-phase/Quadrature). The I/Q mixer produces the two pulses with a phase-difference of $\pi/2$ to get the x and y rotations. The angle of each rotation is set by choosing the time of the pulse. The x pulse (π rotation) is twice longer than the y pulse ($\pi/2$ rotation).

2.2 Universal two-qubit gates

In this section, we will go deeper inside the idea of the fast realization of paradigmatic operations for quantum computing. We will focus now on two-qubit operations and especially on the controlled-phase (CPHASE), the iSWAP and the $\sqrt{\text{iSWAP}}$ gates. For each of them, we will present an implementation protocol exclusively in the resonant regime. Because it is not possible to implement these gates in a fast way directly between two SCqubits, the resonator will play the role of a mediator for the operation. The idea is to map the state of one of the qubits into the cavity-qubit (i.e the first two states of the cavity mode), then to implement the required operation between the cavity and the SCqubit and finally to map back the state of the cavity qubit into the second SCqubit. Another key tool to implement these operations is the use of an auxiliary excited level for one of the SCqubits. The use of three-level physics is inspired by quantum optics and trapped ions where it has already been widely used. We will present some beautiful examples in order to illustrate our motivation. However, in a SCqubit, having a third useful excited level is not obvious. We have to engineer it, that means that we have to find values for the parameters E_J, E_C and N_g different for each type of SCqubit that provide a sufficient anharmonicity between the first four excited levels. This will guarantee us that we do not reach other transitions when we tune on resonance a specific transition among the first three levels of the qubit.

2.2.1 Three-level physics

Three-level physics is a tool widely used in trapped atoms and trapped ions. Some phenomena cannot be observed without using a third level in the atomic system instead of the usual two.

As a first motivation, we will mention the Raman excitations or schemes observed in

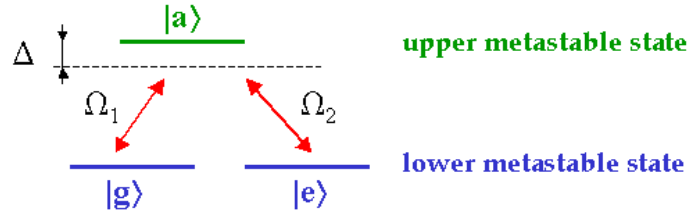trapped ions [22, 23]. A scheme of the system is shown in Fig. 2.7.

Figure 2.7: Raman excitations. One laser Ω_1 tries to excite the level $|a\rangle$ from the level $|g\rangle$ whereas another laser Ω_2 tries to do it from the level $|e\rangle$. Finally, this aims at rotating the qubit $\{|g\rangle, |e\rangle\}$ with a coupling rate $\Omega_1\Omega_2/\Delta$. This would not have been possible without the auxiliary level $|a\rangle$. A direct transition from $|g\rangle$ to $|e\rangle$ is not possible at optical frequencies.

The physical system consists of two metastable multiplets of hyperfine levels of ions. Thanks to the auxiliary level $|a\rangle$ which is a hyperfine level of the upper metastable state, one manages to get a qubit made of two states from the lower metastable state. Because the qubit belongs to this metastable state, it has huge decoherence times which can go from few hours to one day!
The third level is essential because it is not possible to excite $|e\rangle$ from $|g\rangle$ directly because they belong to the same metastable multiplet. And it is not possible to take for the qubit the levels $|g\rangle$ and $|a\rangle$ because it is possible to pass from one to the other by an optical transition which has a fast decay, about 10^{-8}s. Thus it can not be used as a two-level system.

A second example is the adiabatic passage observed in neutral trapped atoms [24, 25]. They succeeded in rotating a qubit formed of two levels from trapped atoms with the help of a third level. The sytem is composed of three states $|g\rangle, |e\rangle, |c\rangle$ as drawn in Fig. 2.8. They use two lasers with different coupling strengths Ω_1 and Ω_2.
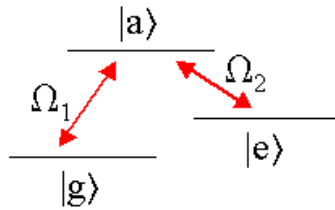

Figure 2.8: Adiabatic passage. They rotate the qubit $\{|g\rangle, |e\rangle\}$ by exciting adiabatically the auxiliary level $|a\rangle$ with laser Ω_1 from level $|g\rangle$ whereas the laser Ω_2 excites it continuously from the level $|e\rangle$.

At the beginning, the strength Ω_2 of the second laser is fixed and the strength of the first laser is small: $\Omega_1 \ll \Omega_2$. The initial state of the system is $|g\rangle$. Then they increase slowly (adiabatically) the first laser. The effect will be to get a superposition of states $|g\rangle$ and $|e\rangle$ which would not have been possible without the auxiliary level. The expression of the qubit state becomes $\frac{\Omega_2}{\sqrt{\Omega_1^2+\Omega_2^2}}|g\rangle + \frac{\Omega_1}{\sqrt{\Omega_1^2+\Omega_2^2}}|e\rangle$.

These applications illustrate how powerful can be the use of a third level. However one has to be careful because it is not so obvious that it can be done experimentally in Circuit

QED. However some groups have already worked on Raman excitations and adiabtic passage [26, 27]. One has to be sure that the anharmonicity of the first four excited levels is strong enough in order to prevent qubit operations from exciting other transitions in the system.

This can be done with a numerical simulation that will give us the regions where the typical parameters of a SCqubit, the ratio E_J/E_C and the gate charge N_g, have values for which all levelspacings are different enough. The program is explained in the appendix A. It is only valid for the charge and transmon SCqubits and displays qualitative results. The plots we got confirm that it should be in fact possible to reach experimentally parameters where the use of a third level is allowed.
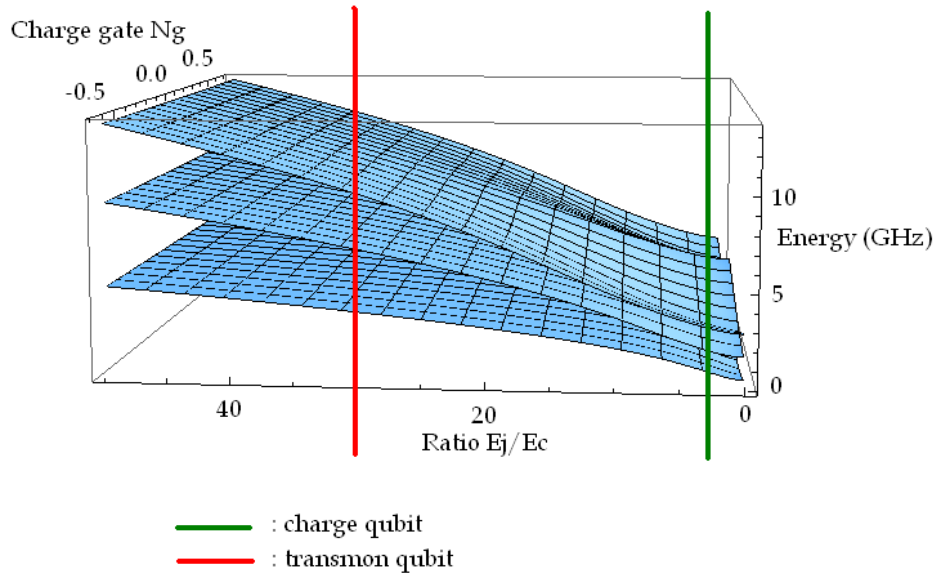

Figure 2.9: Plots of the energies for the first three excited levels of the Hamiltonian valid for the charge and transmon qubits. For each value of E_J/E_C and for each value of N_g, the energy has been renormalized to the ground state's energy. These plots show the anharmonicity of the levels in function of two parameters: the charge gate N_g and the ratio E_J/E_C that defines the type of SCqubit. The red line is drawn at $E_J/E_C = 30$ corresponding to the transmon qubit and the green line is drawn at $E_J/E_C = 3$ corresponding to the charge qubit. The goal is to find a value near $N_g = 0,5$ for which the anharmonicty is strong enough for both types of SCqubits. In this case the use of an auxiliary level will be allowed.

We will now present three universal two-qubit gates and the engineered protocols to implement them fast.

2.2.2 The controlled-phase (CPHASE) gate

The controlled-phase (CPHASE) gate is a two-qubit gate defined as:

$$|a,b\rangle \xrightarrow{\text{CPHASE}} e^{i\pi\delta_{a1}\delta_{b1}}|a,b\rangle, \tag{2.25}$$

where the states $|a\rangle$ and $|b\rangle$ are one of the eigenstates $\{|0\rangle, |1\rangle\}$ and δ_{a1} and δ_{b1} are the Kronecker deltas.

In the basis $\{|00\rangle, |01\rangle, |10\rangle, |11\rangle\}$, its matrix is:

$$\text{CPHASE} = \begin{pmatrix} 1 & 0 & 0 & 0 \\ 0 & 1 & 0 & 0 \\ 0 & 0 & 1 & 0 \\ 0 & 0 & 0 & -1 \end{pmatrix}$$

It means that the state $|11\rangle$ where the two qubits are in their excited level will be phase-shifted by an angle π and the other states do not change.

The CPHASE gate is interesting because it can be used with other one-qubit gates to form a set of universal gates. Historically, the CPHASE gate was first implemeted in Cavity QED by the group of S. Haroche in ENS Paris between a cavity-qubit (electromagnetic field with one or zero photon) and an atom-qubit which was a single Rydberg atom [28]. They used an auxiliary level to implement the operation and this result motivated our present proposal.

In our context of Circuit QED we are interested in performing a CPHASE gate between two SCqubits in a resonator. One possible experimental realization is that of [29] shown in Fig. 2.10.
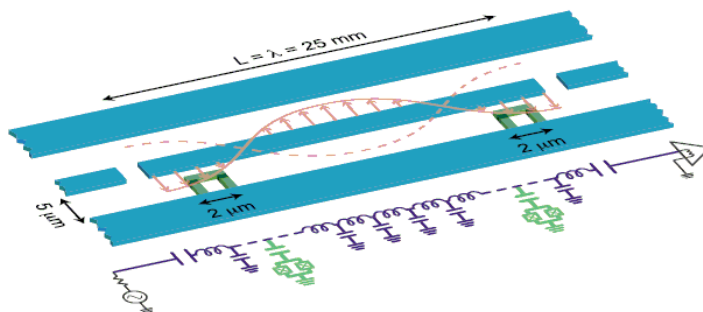

Figure 2.10: Experimental setup with two SCqubits inside a 1D-resonator. Illustration taken from [29].

The system is composed of:

- one cavity-qubit $\{|0\rangle, |1\rangle\}$, which corresponds to a resonator field with 1 or 0 photons.

- two SCqubits $\{|g_1\rangle, |e_1\rangle\}$ and $\{|g_2\rangle, |e_2\rangle\}$ with an auxiliary excited level for each qubit $|a_1\rangle$ and $|a_2\rangle$. Let us note that for one operation between two qubits, we will use only one auxiliary level.

The interaction between each qubit and the cavity is possible by tuning on resonance the transition frequencies we need with the cavity-qubit. Supposing that each transition frequency in each qubit is different, the corresponding coupling constants are different too. A scheme of the experimental setup with the transition frequencies we need for this gate is shown in Fig. 2.11.

In the initial state both SCqubits are in a superposition state and the cavity has 0 photons. The general state is:

$$|\Psi_i\rangle = \Big(\alpha \, |g_1 g_2\rangle + \beta \, |g_1 e_2\rangle + \gamma \, |e_1 g_2\rangle + \delta \, |e_1 e_2\rangle\Big) \otimes |0\rangle. \tag{2.26}$$
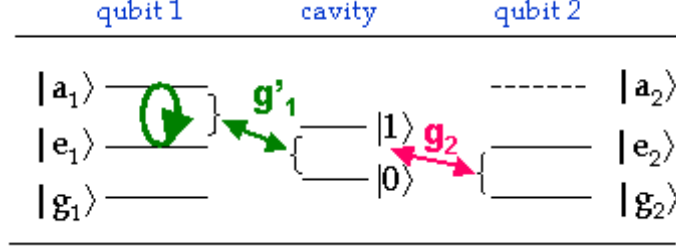
Figure 2.11: Scheme for the implementation of the CPHASE gate.

As explained before, the two main ideas to implement this gate in Circuit QED in a fast way are to use the cavity as a mediator [30] and to use an auxiliary excited level for one of the SCqubit. Therefore we will first map the second SCqubit into the cavity qubit, then we will implement the CPHASE gate between the first SCqubit and the cavity using an auxiliary level for the SCqubit, and finally we will map back the cavity qubit into the second SCqubit to get the operation between both SCqubits. The exact manipulations between the SCqubits and cavity are described in Fig. 2.12 and the detailed protocol can be found below.

Step	Required transitions	Coupling constant	Pulse
i) Mapping	$(\lvert g_2\rangle, \lvert e_2\rangle) \longrightarrow (\lvert 0\rangle, \lvert 1\rangle)$	g_2	π-pulse
ii) CPHASE gate	$(\lvert e_1\rangle, \lvert a_1\rangle) \longleftrightarrow (\lvert 0\rangle, \lvert 1\rangle)$	g'_1	2π-pulse
iii) Back mapping	$(\lvert g_2\rangle, \lvert e_2\rangle) \longleftarrow (\lvert 0\rangle, \lvert 1\rangle)$	g_2	π-pulse

Figure 2.12: Protocol to implement the CPHASE gate between two SCqubits in a cavity.

Applying the protocol explained in Fig. 2.12 on the initial step, we get the following final step:

$$|\Psi_f\rangle = \left(\alpha\,|g_1 g_2\rangle + \beta\,|g_1 e_2\rangle + \gamma\,|e_1 g_2\rangle - \delta\,|e_1 e_2\rangle\right) \otimes |0\rangle \qquad (2.27)$$

which corresponds exactly to what a CPHASE gate does: the state where both qubits are excited has now a minus sign whereas the other states did not change. We see that the use of the third level was crucial to implement in a few steps this logical gate using only resonant couplings. It would not have been possible without it.

Detailed protocol for the CPHASE gate

At the beginning the cavity field has 0 photon which corresponds to the state $|0\rangle$ and both SCqubits are in the superposition states $\frac{1}{\sqrt{2}}(|g_1\rangle + |e_1\rangle)$ and $\frac{1}{\sqrt{2}}(|g_2\rangle + |e_2\rangle)$ which can be obtained by performing a fast Hadamard gate or a y rotation. The initial state of all the system is thus

$$|\Psi_0\rangle = \left(\alpha\,|g_1 g_2\rangle + \beta\,|g_1 e_2\rangle + \gamma\,|e_1 g_2\rangle + \delta\,|e_1 e_2\rangle\right) \otimes |0\rangle \qquad (2.28)$$

i) First step: we want to use the cavity as mediator

For this we have to map the second SCqubit into the cavity-qubit. The qubit 2 and the resonator are tuned on resonance with the coupling constant g_2 for a π-pulse. To put in resonance both system, we change the transition frequency using additional control lines reaching each qubit. As a result a mapping of the second SCqubit onto the resonator qubit is performed and can be described as following:

$$|\Psi_1\rangle = \Big(\alpha\,|g_1 0\rangle + \beta\,|g_1 1\rangle + \gamma\,|e_1 0\rangle + \delta\,|e_1 1\rangle\Big) \otimes |g_2\rangle \qquad (2.29)$$

The cavity contains at this step one or zero photon and it will be possible to perform the well-known CPHASE gate between the cavity and the first qubit.

   ii) Second step: CPHASE gate between the first qubit and the cavity qubit according to the realization in Cavity QED [28].

The qubit $\{|e_1\rangle, |a_1\rangle\}$ and the cavity are tuned on resonance via the coupling g_1' for a 2π-pulse. The SCqubit-resonator system undergoes a reversible Rabi-oscillation. The global state inside the cavity is now:

$$|\psi_1\rangle \overset{2\pi-pulse}{\to} |\psi_2\rangle = \Big(\alpha\,|g_1 0\rangle + \beta\,|g_1 1\rangle + \gamma\,|e_1 0\rangle - \delta\,|e_1 1\rangle\Big) \otimes |g_2\rangle. \qquad (2.30)$$

   iii) Third step: CPHASE between the two SCqubits through a mapping back.

At this stage the CPHASE gate has been done between the first qubit and the cavity. Our aim is to implement this logical operation between the two qubits. To reach it, we have to map back the cavity-qubit onto the second qubit. This "back mapping" can be done via tuning on resonance once again the second qubit $\{|g_2\rangle, |e_2\rangle\}$ and the resonator with the coupling g_2 for a π-pulse. The resulting state is:

$$|\psi_2\rangle \overset{\pi-pulse}{\to} |\psi_3\rangle = \Big(\alpha\,|g_1 g_2\rangle + \beta\,|g_1 e_2\rangle + \gamma\,|e_1 g_2\rangle - \delta\,|e_1 e_2\rangle\Big) \otimes |0\rangle. \qquad (2.31)$$

Summary

Thanks to this protocol conceived to implement the CPHASE gate in a fast way and the universal one-qubit gates, we possess at this stage all the required tools to perform standard quantum computing in Circuit QED with resonant gates.
Nevertheless because the iSWAP and $\sqrt{\text{iSWAP}}$ are widely used as universal two-qubit gates, we will present a protocol also exclusively in the resonant regime for each of them. Concerning the CNOT gate, it can be decomposed by using the Hadamard and CPHASE gates as shown in Appendix B so we will not detail the realization of this gate here.

2.2.3   The iSWAP and $\sqrt{\text{iSWAP}}$ gates

The iSWAP and $\sqrt{\text{iSWAP}}$ are very useful to implement lots of algorithms or to construct other two-qubit gates. However they have been implemented until now only in the dispersive regime using the flip-flop interaction Hamiltonian Ref. [29, 31] for which they occur naturally. In this section we will give their implementation with only fast resonant steps. Whereas the

implementation of the CPHASE gate was inspired from quantum optics, these protocols are completely new. We use the same tools, the cavity as mediator and a third level but the protocol is more sophisticated and requires another transition frequency of the first qubit. We will show that we can implement the iSWAP and $\sqrt{\text{iSWAP}}$ gates in five steps using only resonant couplings.

The iSWAP and $\sqrt{\text{iSWAP}}$ gates

The corresponding matrices are respectively [30]:

$$\text{iSWAP} = \begin{pmatrix} 1 & 0 & 0 & 0 \\ 0 & 0 & i & 0 \\ 0 & i & 0 & 0 \\ 0 & 0 & 0 & 1 \end{pmatrix} \quad \sqrt{\text{iSWAP}} = \begin{pmatrix} 1 & 0 & 0 & 0 \\ 0 & \frac{1}{\sqrt{2}} & \frac{i}{\sqrt{2}} & 0 \\ 0 & \frac{i}{\sqrt{2}} & \frac{1}{\sqrt{2}} & 0 \\ 0 & 0 & 0 & 1 \end{pmatrix}$$

The iSWAP operation is equivalent to the CNOT gate up to one-qubit gates but with an additional phase i. The CNOT gate has for effect to exchange the states of the second qubit or target-qubit if the first qubit or control-qubit is in state $|1\rangle$. The $\sqrt{\text{iSWAP}}$ has for effect to rotate both qubits too but with a different phase. Therefore it can be implemented with the same protocol, we have just to be careful to rotate the first qubit for a $\pi/2$-pulse instead of a π-pulse for the iSWAP. This will be specified in more detal in the protocol.

As for the CPHASE gate, we will summarize the protocol into a table Fig. 2.14 in order to get the main idea of the steps. The detailed protocol can be found afterwards.
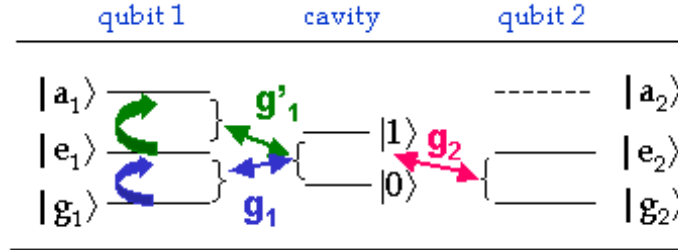

Figure 2.13: Scheme for the implementation of the iSWAP and $\sqrt{\text{iSWAP}}$ gates.

The initial state is:

$$|\Psi_i\rangle = \Big(\alpha\,|\text{g}_1\text{g}_2\rangle + \beta\,|\text{g}_1\text{e}_2\rangle + \gamma\,|\text{e}_1\text{g}_2\rangle + \delta\,|\text{e}_1\text{e}_2\rangle\Big) \otimes |0\rangle. \tag{2.32}$$

The steps described in the table Fig. 2.14 and applied on the initial state lead to the following final state:

$$|\Psi_f\rangle = \Big(\alpha\,|\text{g}_1\text{g}_2\rangle + \beta\,\text{i}\,|\text{e}_1\text{g}_2\rangle) + \gamma\,\text{i}\,|\text{g}_1\text{e}_2\rangle + \delta\,|\text{e}_1\text{e}_2\rangle\Big) \otimes |0\rangle. \tag{2.33}$$

which corresponds exactly to the iSWAP gate with only resonant operations between two SCqubits inside the same resonator. Because it is a new proposal we will compare the time required for the implementation of the $\sqrt{\text{iSWAP}}$ gate following our protocol to the time needed for a realization in the off-resonant regime. Experimentally, the dispersive implementation

Step	Required transitions	Coupling constant	Pulse
i) Mapping	$\{|g_2\rangle, |e_2\rangle\} \longrightarrow \{|0\rangle, |1\rangle\}$	**g_2**	π-pulse
ii) Shelving	$\{|e_1\rangle, |a_1\rangle\} \longleftrightarrow \{|0\rangle, |1\rangle\}$	**g'_1**	π-pulse
iii)Rotation of qubit 1	$\{|e_1\rangle, |a_1\rangle\} \longleftrightarrow \{|0\rangle, |1\rangle\}$	**g_1**	iSWAP: π-pulse $\sqrt{}$iSWAP: $\pi/2$-pulse
iv) Back shelving	$\{|e_1\rangle, |a_1\rangle\} \longleftrightarrow \{|0\rangle, |1\rangle\}$	**g'_1**	$(-\pi)$-pulse
v) Back mapping	$\{|g_2\rangle, |e_2\rangle\} \longleftarrow \{|0\rangle, |1\rangle\}$	**g_2**	π-pulse

Figure 2.14: Protocol to implement the iSWAP gate between two SCqubits in a cavity.

can be done with the experimental setup of the Yale group [23] in one step with a $\pi/4$-pulse. The corresponding rate is thus: $t_{\text{disp}} = \frac{\pi \Delta}{4g^2}$. In our case, we put equal to g the coupling constants for simplicity. This leads to the time: $t_{\text{off}} = \frac{5\pi}{g}$. We can observe that our protocol is efficient when we have at least a dispersive regime characterized by $\Delta \geq 20g$. Theoretically the large detuning occurs when $\Delta \approx 100g$. In this case our proposition is really much better than the off-resonant regime. As a consequence, if one works experimentally with a small detuning, the time of the realization does not change depending to the regime in which you are. However if one supposes a strong detuning in your system, then it is really better to use our proposal.

Detailed protocol for the iSWAP and $\sqrt{\text{iSWAP}}$ gates

Let us mention that the protocols for implementing the iSWAP and $\sqrt{\text{iSWAP}}$ gates follow similar steps. The initial state is:

$$|\Psi_0\rangle = \left(\alpha |g_1 g_2\rangle + \beta |g_1 e_2\rangle + \gamma |e_1 g_2\rangle + \delta |e_1 e_2\rangle \right) \otimes |0\rangle \qquad (2.34)$$

i) We want use the cavity qubit as mediator. Therefore, we map the second qubit into the cavity by tuning on resonance the levels $\{|g_2\rangle, |e_2\rangle\}$ with the cavity $|0\rangle$ via the coupling constant g_2. We perform a π-quantum Rabi pulse.
The resulting state is:

$$|\Psi_1\rangle = \left(\alpha |g_1 0\rangle + \beta |g_1 1\rangle + \gamma |e_1 0\rangle + \delta |e_1 1\rangle \right) \otimes |g_2\rangle. \qquad (2.35)$$

ii) We want to shelve the population of the excited level of the first qubit $|e_1\rangle$ to the auxiliary level $|a_1\rangle$ in order to be free to rotate the population of the ground state of the first qubit $|g_1\rangle$ without reaching other levels.
We implement this population transfer by coupling the levels $\{|e_1\rangle, |a_1\rangle\}$ with the cavity via the coupling constant g'_1 and perform a π-quantum Rabi pulse.

We get:

$$|\Psi_2\rangle = \left(\alpha |g_1 0\rangle + \beta |g_1 1\rangle + \gamma |e_1 0\rangle + \delta |a_1 0\rangle \right) \otimes |g_2\rangle. \qquad (2.36)$$

iii) We want now to rotate the first qubit. The difference between the iSWAP and $\sqrt{\text{iSWAP}}$ gates is at this step. For the iSWAP gate, we tune on resonance the qubit $\{|g_1\rangle, |e_1\rangle\}$ and

the cavity via the coupling constant g_1 for a π-quantum Rabi pulse. The global phase has to be set to $\phi = 0$. Whereas for the $\sqrt{\text{iSWAP}}$ gate, we tune this transition frequency with the cavity for a $\pi/2$-quantum Rabi pulse with the same global phase $\phi = 0$. For the iSWAP gate, we will obtain the state:

$$|\Psi_3\rangle = \Big(\alpha\,|g_10\rangle + \beta\,\mathrm{i}\,|e_10\rangle) + \gamma\,\mathrm{i}\,|g_11\rangle + \delta\,|a_10\rangle\Big) \otimes |g_2\rangle. \tag{2.37}$$

iv) We have now the logical operation corresponding to the iSWAP gate but between the first qubit and the cavity-qubit. To get it between the two SCqubits, we have to do the inverse population transfer and the back mapping.

The inverse qubit transfer can be done by tuning on resonance the transition $\{|e_1\rangle, |a_1\rangle\}$ with the cavity via the coupling constant g_1' for a $(-\pi)$-quantum Rabi pulse. The back mapping is implemented by tuning on resonance again the second qubit $\{|g_2\rangle, |e_2\rangle\}$ and the cavity with the coupling g_2 for a π-quantum Rabi pulse.

The final state for the iSWAP gate is:

$$|\Psi_{\text{final}}\rangle = \Big(\alpha\,|g_1g_2\rangle + \beta\,\mathrm{i}\,|e_1g_2\rangle) + \gamma\,\mathrm{i}\,|g_1e_2\rangle + \delta\,|e_1e_2\rangle\Big) \otimes |0\rangle. \tag{2.38}$$

Summary

Using always the same experimental setup and one auxiliary level, we are able to implement all the most important two-qubit operations in a resonant way. In the next chapter we will apply these new experimental possibilities to two research fields: one-way quantum computing and strongly correlated systems. One-way quantum computing is an alternative scalable quantum computer proposed several years ago. One of the requirement is to work on a particular entangled state, the cluster state. Our goal will be to implement it in Circuit QED using the two-dimensional cavity grid in an optimal way, again with resonant operations. A second application concerns the simulation of strongly correlated systems. We will concentrate on the XX and Ising models using a very new theoretical approach. The idea consists in simulating these models in Circuit QED with the help of quantum circuits. After explaining the arguments leading to this method, we will implement the gates required in these circuits using only resonant steps.

Chapter 3

Application to one-way quantum computing

In this chapter we will present a protocol to implement a cluster state in the two dimensional cavity grid with the resonant operations discussed in the last chapter. A cluster state is a particular multiqubit entangled state that will be defined below. It constitutes the first step towards the realization of a scalable one-way quantum computer [32, 33]. We will show that for N^2 qubits in the cavity-grid, the time to get the cluster state scales with N. First we will expose the main ideas of one-way quantum computing which constitutes an alternative to standard quantum computing. Then we will define the cluster state and finally we will present its protocol of implementation specific to Circuit QED in the 2D-cavity grid.

3.1   Review of one-way quantum computing

The principle of standard quantum computing is based on producing and exploiting entanglement during the computation process. The information is written on an input state, then operations and measurements are performed and the final result is read out. The main characteristic of one-way quantum computing is that the entire resource of entanglement is provided by the initial state. The quantity of entanglement thus decreases with every measurement. This has to be compared to schemes where measurements, such as Bell measurements, are able to create entanglement during the process. In a one-way quantum computer the initial state is a cluster state whose number of qubits defines its class of entanglement. For instance, a cluster state of three qubits belongs to the GHZ class, whereas a cluster state of four qubits belongs neither to the GHZ nor to the W class [34, 35, 36]. Another distinction of one-way quantum computing is that only one-qubit measurements are required. It has been shown that any quantum circuit can be imprinted by one-qubit measurements on a cluster state [32].

More precisely, quantum computation on a cluster state according to the principles of one-way quantum computing works as follows: An input state is implemented on the cluster state by performing σ_z measurements on a set of qubits. Then the remaining qubits are measured in an certain order and in a certain basis. The basis depends on the results of the preceding measurements. This allows to propagate the information horizontally in the cluster and two-qubit operations are performed vertically as shown in Fig. 3.1. The final state is read out by measuring the last qubit on each "wire".
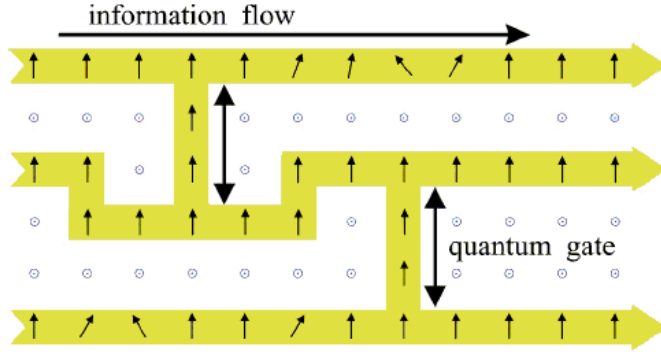
Figure 3.1: Example of one-way quantum computing. The circles symbolize measurements in the σ_z basis and are used to implement the initial state. The information is propagated horizontally by performing measurements in the σ_x basis (vertical arrows) and measurements in the x-y plane (tilted arrows). The state is finally read out on the last free qubit on each wire. Illustration taken from [32].

In the next section, we will define the cluster state in one and two dimensions and see how it can be constructed theoretically. Finally, we will present a protocol to implement it in Circuit QED in the two dimensional cavity grid in a fast way. We will consider the case where the cavity-array contains N^2 SCqubits. Because we already know how to perform certain two-qubit gates in the resonant regime as discussed in the last chapter, we will try to use them to optimize the construction of this specific entangled state.

3.2 Cluster states

Topological definition [33]

Given a lattice of dimension d and the subset $\mathcal{A} \subset \mathbb{Z}$ of all sites of the lattice occupied by a qubit, a cluster $\mathcal{C} \subset \mathcal{A}$ is a subset of $\mathcal{A}$ obeying the following properties:

- any two sites c and c' $\in \mathcal{C}$ are connected

- any sites $c \in \mathcal{C}$ and $a \in \mathcal{A} \backslash \mathcal{C}$ are not connected

where the term "two qubits are connected" means that there exists a consecutive sequence of occupied neighbouring sites between both qubits.

Mathematical expressions

In one dimension, a cluster state of N qubits corresponds to a maximally entangled chain and is defined as:

$$|\Phi_N\rangle = \frac{1}{2^{N/2}} \bigotimes_{c=1}^{N} \left(|0\rangle_c + |1\rangle_c \sigma_z^{c+1} \right), \tag{3.1}$$

where σ_z is the Pauli matrix and σ_z^{c+1} acts on the qubit at site c+1.

To illustrate this definition, let us give the expression of a cluster state formed of three qubits where each qubit can be one of the states $\{|0\rangle, |1\rangle\}$.

$$|\Phi_3\rangle = |000\rangle + |001\rangle + |010\rangle - |011\rangle + |100\rangle + |101\rangle - |110\rangle + |111\rangle \qquad (3.2)$$

Recalling the logical operation of the resonant CPHASE gate, we may notice immediately that it is rigorously the same state which we would have obtained implementing a CPHASE gate between the neighbouring qubits of a 1D-chain composed of three qubits. The states with two neighbour qubits in state $|1\rangle$ are π-phase shifted, which explains the sign minus in front of them. When there are two pairs of neighbour qubits in state $|1\rangle$, both minus signs cancel, which explains the sign plus in front of the state $|111\rangle$. As we know how to perform the CPHASE gate fast, this equivalence will be the key point in the implementation of a cluster state in Circuit QED. One can remark that the order of the operations does not matter. Mathematically this is proven noting that the commutator $\left[\sigma_z^a, \sigma_z^b\right] = 0$, where a and b denote different qubits.

In a two-dimensional space, a cluster state is defined as:

$$|\Phi_N\rangle = \frac{1}{2^{N/2}} \bigotimes_{c \in \mathcal{C}} \left(|0\rangle_c + |1\rangle_c \otimes_{\gamma \in \Gamma} \sigma_z^{c+\gamma}\right),$$

where

- Γ stays for the basis of the lattice. For instance if $d = 2$, $\Gamma = \{(1,0), (0,1)\}$,

- $\mathcal{C}$ denotes the set of SCqubits belonging to the cluster,

- if $c + \gamma \notin \mathcal{C}$, then $\sigma_z^{c+\gamma} = 1$,

- $c + \gamma > c$.

It can be proved that in two dimensions the equivalence with the CPHASE gate is still valid. Indeed considering always CPHASE operations between neighbour qubits, it does not matter in which direction and in which order we first perform the gate. We only have to be careful not to perform the gate between two diagonal qubits. We give here an example of a cluster state in two dimensions composed of four qubits $|\Phi_4\rangle$. The notation for a state is $|1\,2\,3\,4\rangle$ according to the notation of Fig. 3.2 .

$$
\begin{aligned}
|\Phi_4\rangle \;=\;& |0000\rangle + |0001\rangle + |0010\rangle - |0011\rangle + |0100\rangle - |0101\rangle + |0110\rangle + |0111\rangle + \\
+\;& |1000\rangle + |1001\rangle - |1010\rangle - |1011\rangle - |1100\rangle + |1101\rangle + |1110\rangle + |1111\rangle \qquad (3.3)
\end{aligned}
$$

One can explain the signs of this state with the same rules as in one dimension and being careful not to entangle diagonal qubits. We can remark that the order in which we entangle the qubits is not important.

We will now present how a cluster state can be built from a theoretical point of view. In the initial state all qubits should be in a superposition state that can be realized by performing a Hadamard gate or a y rotation on each of them. The state is:

$$|\Psi_{in}\rangle = \bigotimes_{a=1}^{N} \left(\frac{|0\rangle_a + |1\rangle_a}{\sqrt{2}}\right). \qquad (3.4)$$
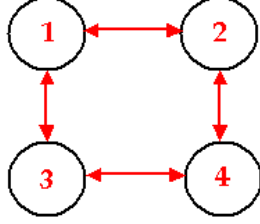
Figure 3.2: Two dimensional cluster states with four qubits. A nearest-neighbour interaction entangle them, which can be implemented with a CPHASE gate or by applying the evolution operator of the Ising model for a specific time - Eq.(3.7).

Then we make the neighbour qubits interact via an Ising interaction. In one dimension the Hamiltonian describing the Ising model with the restriction of nearest-neighbour interactions is:

$$H_{\text{Ising}} = \hbar g \sum_{\substack{a,b \in C \\ b-a=1}} \Big(\frac{1-\sigma_z^a}{2}\Big)\Big(\frac{1-\sigma_z^b}{2}\Big),$$

where g is the strength of the short-range interaction.

In two dimensions it is:

$$H_{\text{Ising}} = \hbar g \sum_{a,a'} f(a - a')\Big(\frac{1-\sigma_z^a}{2}\Big)\Big(\frac{1-\sigma_z^{a'}}{2}\Big), \tag{3.5}$$

where

- the indices a and a' run over all occupied sites of the lattice (site $a \in \mathbb{Z}^d$),

- $f(a - a')$ specifies the interaction range. Here it is a next-neighbour interaction represented by $f(a - a') = \delta^{(2)}_{a+1,a'}$.

For simplicity we will use the Hamiltonian in one dimension in the next explanations but it would be the same with the Hamiltonian in two dimensions. The corresponding evolution operator S_{Ising} is:

$$
\begin{aligned}
S_{\text{Ising}} &= e^{-\frac{i}{\hbar}H_{\text{Ising}}t} = e^{-igt \sum \left(\frac{1-\sigma_z^a}{2}\right)\left(\frac{1-\sigma_z^b}{2}\right)} \\
&= \prod_{\substack{a,b \in C \\ b-a=1}} \exp(-i\frac{gt}{4}) \exp(i\frac{gt}{4}\,\sigma_z^a) \exp(i\frac{gt}{4}\,\sigma_z^b) \exp(-i\frac{gt}{4}\,\sigma_z^a\sigma_z^b).
\end{aligned}
\tag{3.6}
$$

To get the same expression of a cluster state as in Eq. (3.1), we have to choose t so that gt is equal to π. The unitary operation required to get a cluster state in one dimension is thus:

$$S_{\text{cluster}} = \prod_{\substack{a,b \in C \\ b-a=1}} \exp(-i\frac{\pi}{4}) \exp(i\frac{\pi}{4}\,\sigma_z^a) \exp(i\frac{\pi}{4}\,\sigma_z^b) \exp(-i\frac{\pi}{4}\,\sigma_z^a\sigma_z^b). \tag{3.7}$$

Now we can implement theoretically the interaction between the neighbour qubits in a superposition state by applying this evolution operator on the initial state Eq. 3.4. It will lead to the cluster state. We can note that all the operators in the evolution operator S_{cluster} commute. This means that it is at least mathematically possible to apply it simultaneously on all neighbour qubits of the system. However, experimentally it depends on the physical system we work with. In our case it is the two-dimensional cavity grid and we will see that it does not allow the simultaneous realization of all gates.

Summary

On the one hand, we explained how a cluster state in one and two dimensions can be built by implementing an Ising interaction between neighbour qubits. On the other side, considering the definition of a cluster state, we became aware that it is equivalent to the state obtained after performing the CPHASE gate between all neighbour qubits in a superposition state initially in one and two dimensions. Fortunately we discussed in the last chapter the fast realization of the CPHASE gate. This gives us the key idea to write a physical implementation of the cluster state in Circuit QED using resonant operations.

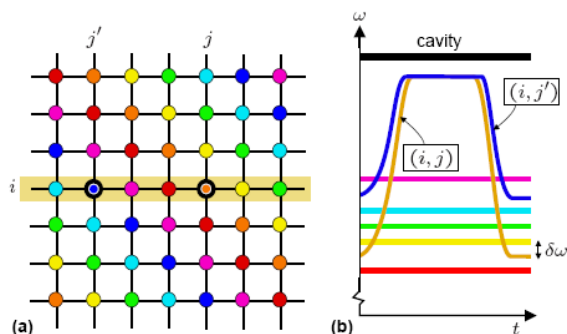## 3.3   Two-dimensional cluster state in a cavity grid

Figure 3.3: a) Architecture of a 2D cavity grid. Each line represents a one-dimensional resonator presented before and qubits which are denoted with circles are situated at the crossing point of two cavities. In a given cavity each qubit has a different transition frequency which can be changed by playing with the parameters of the qubit. b) Two qubits can be tuned into mutual resonance by changing their transition frequencies. Illustration taken from [18].

We recall the setup of the two-dimensional cavity grid in Fig.3.3. We consider N^2 SC-qubits in this cavity grid. We will need two types of operations: the y rotation and the CPHASE gate. Their definition and their fast implementation are described in chapter 2. As explained in the last section, we will need to implement first a rotation around the y axis of a $\pi/2$ angle on each qubit to put them in a superposition state. We could use the Hadamard gate but even with our new proposal it would require two pulses instead of one so we stay with the y rotation solution. Then we will have to implement the required interaction between all neighbour qubits of the grid via CPHASE gates. The goal is to reduce as much as possible the

total time of the implementation. This is done on the one side by using resonant operations and on the other side by performing simultaneously all the gates we can, taking into account the constraints given by the architecture of the cavity array. At the beginning all the qubits are in the initial state $|0\rangle$.

The first step consists in performing simultaneous y rotations on all the qubits to put them in the superposition state. Experimentally the simultaneity is possible because the y rotation is a local operation. Thanks to the setup we will be able to tune on resonance each qubit with its own external driving field which contains the $\pi/2$-pulse required for the operation. The resulting global state will be:

$$|\Psi_{in}\rangle = \bigotimes_{c=1}^{N} \frac{|0\rangle_c + |1\rangle_c}{\sqrt{2}} \quad \forall c \in \mathcal{C}. \tag{3.8}$$

The total time needed for this operation can take two forms. One solution is to consider that all the rotations can be implementd simultaneously and then the time will be independant of N: $\tau = \frac{\pi}{2\Omega_R}$, where Ω_R is the coupling constant between the external driving field and the SCqubit. However, with the actual setup of the cavity grid, this would require one microwave generator for each qubit, an expensive solution that would demand N^2 generators.
Another solution is to perform this operation in N steps. In this case we would send one microwave generator that will act on one qubit in each cavity and repeat it N times. This solution would be linear with N and we will consider this one to be the more reasonable possible for the realization of the cluster state. The corresponding time is:

$$\tau_1 = N \cdot \frac{\pi}{2\Omega_R}. \tag{3.9}$$

In the second step we have to implement all CPHASE gates between neighbour qubits. At this stage, we have to consider the architecture of the cavity grid which will imply that we cannot perform all the operations simultaneously. It can be explained by the following fact. Each cavity contains zero or one photon according to the setup needed for the CPHASE gate. The realization of this gate between two qubits inside one cavity requires the use of the cavity qubit. The constraint is thus to never perform more than one CPHASE gate in one cavity. This leads to the following proposition.

i) Simultaneous CPHASE gates

We can perform all CPHASE gates on the first row using the vertical cavities plus the ones we can do on the first column with the unused horizontal cavities. We can repeat this step N times moving the row and the column to the top and the right in order to cover all the cavity-grid. As a result we will have implemented all the required CPHASE gates between neighbour qubits except the ones corresponding to the crossing point between the horizontal and vertical cavities during the operation. This is showed in Fig. (3.4).
The time needed to do these N steps is:

$$\tau_2 = N\left(\frac{\pi}{g_2} + \frac{2\pi}{g_1'} + \frac{\pi}{g_2}\right), \tag{3.10}$$

where $\left(\frac{\pi}{g_2} + \frac{2\pi}{g_1'} + \frac{\pi}{g_2}\right)$ is the time needed for one CPHASE gate and g_2 and g_1' are the coupling constants characterizing the strong coupling regime between the transition frequency we want
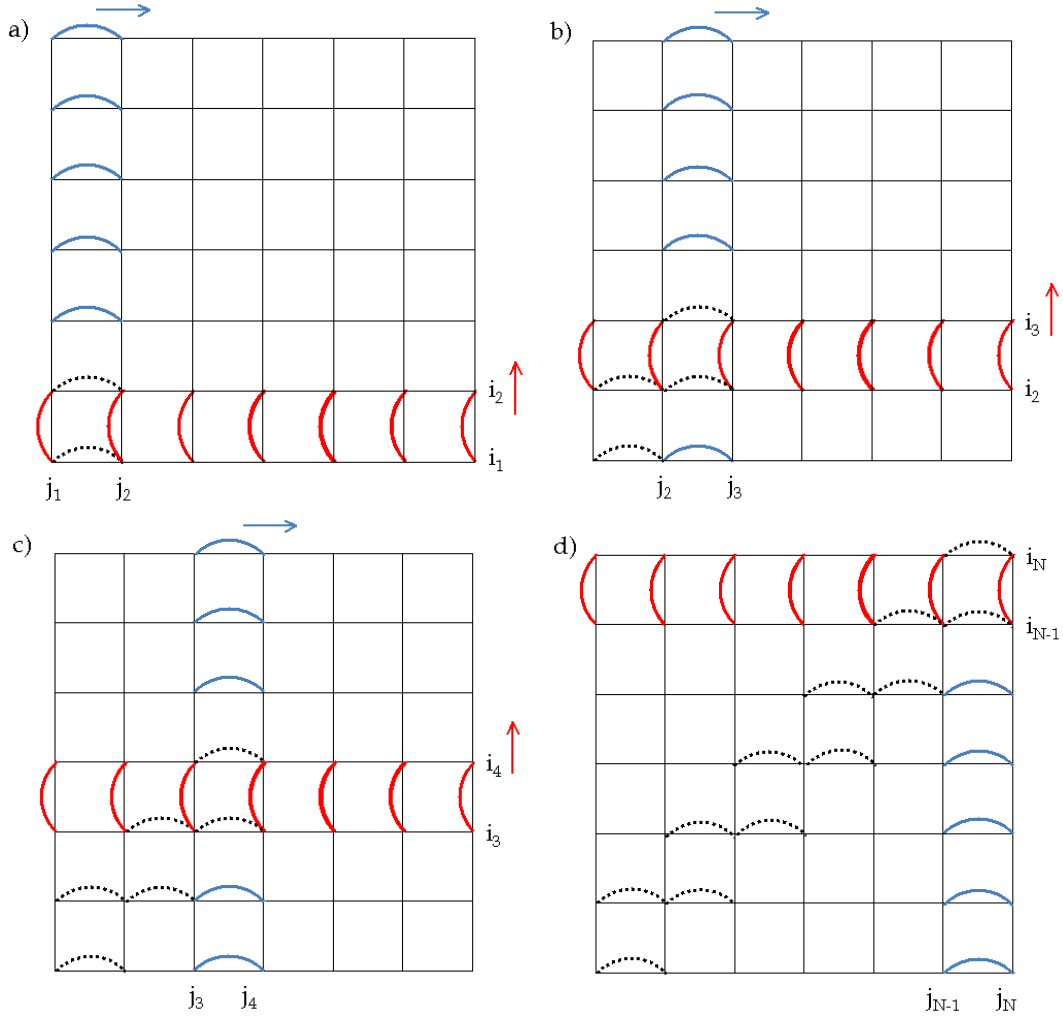
Figure 3.4: Implementation of the simultaneous CPHASE gates in a cavity grid following the steps (a-d). The grid is composed of $N \times N$ cavities and contains N^2 qubits at each crossing point of two cavities. The performed CPHASE gates for the lines are displayed in red and for the columns in blue. The row is shifted to the top and the colum to the right. The missing gates at the crossings are indicated as dashed black lines.

to tune on resonance with the cavity frequency defined in chapter two.

ii) The missing gates

We have now to implement the missing gates situated at the crossing points. In Fig. 3.4, we observe that there are two missing gates in each horizontal cavity. We will have thus to do it in two steps, one diagonal first and the second after. The time needed for this is:

$$\tau_3 = 2\left(\frac{\pi}{g_2} + \frac{2\pi}{g_1'} + \frac{\pi}{g_2}\right). \tag{3.11}$$

At this stage we have applied all CPHASE gates, which means that we have obtained the desired cluster state required for one-way quantum computation. The total time to build it

is:

$$\tau_{tot} = \frac{N \cdot \pi}{2\Omega_R} + N\left(\frac{\pi}{g_2} + \frac{2\pi}{g_1'} + \frac{\pi}{g_2}\right) + 2\left(\frac{\pi}{g_2} + \frac{2\pi}{g_1'} + \frac{\pi}{g_2}\right) \tag{3.12}$$

$$= \frac{N \cdot \pi}{2\Omega_R} + (N+2)\, 2\pi\, (\frac{g_2 + g_1'}{g_2\, g_1'}). \tag{3.13}$$

Thanks to this expression, we see the great advantage of this protocol. We managed to implement a cluster state of N^2 SCqubits with a building-time which scales with N. This result constitutes the first detailed proposal to implement a cluster state in Circuit QED and opens the way to the one-way quantum computer. Moreover it is interesting from an experimental point of view because of the use of only resonant operations in a new architecture for Circuit QED: the 2D-cavity grid.

Summary

In this chapter we were able to use the resonant universal gates engineered in the previous section to build a scalable cluster state in Circuit QED and thus to make a step more in the direction of one-way quantum computing. The main improvement comes from the fact that we were able to implement a particular entangled state of N^2 SCqubits in a time linear in N.

Chapter 4

Application to strongly correlated systems

In this chapter we will base our work on an idea recently proposed by F. Verstraete, I. Cirac and J. I. Latorre [37]. They propose an experimental method to simulate any state, its time evolution and thermal superposition of many states for strongly correlated models by applying a specific unitary transformation on a strictly local Hamiltonian. For instance, they study the XX model and the Ising model in a transverse magnetic field. They give the corresponding unitary operations in the form of quantum circuits composed of two-qubit gates. It should be a great improvement compared to the actual realization of strong interactions in physical systems because it is nowadays an experimental difficulty. The origin of the idea comes from an analytical transformation which will be explained in the next section. They managed to prove that the quantum circuits implementing the required unitary transformation are composed of a finite number of non trivial two-qubit gates. First we will explain in more detail the proposal of F. Verstraete *et al.* and the different required quantum circuits. Finally, we will focus on our aim and present our realizations in the resonant regime of these two-qubit gates using again three-level physics.

4.1 Quantum simulation of strongly correlated systems

In Ref. [37] the authors present a theoretical proposal to reproduce the strong correlations described in the XX and Ising models in Circuit QED and to simulate the quantum evolution of any of those states and the thermal superposition of them.

The mathematical idea is to cast the XX or Ising Hamiltonians into a simple theory with only local terms, which means without any interaction between the elements of the system. They reach this goal by disentangling all the eigenstates of the correlated Hamiltonian by following the analytical transformation. The main steps are mentioned below:

1) The spins (variable σ) are mapped into fermions (variable c).

2) The Fourier Transform is used to get the fermions in the momentum space (variable b).

3) The Bogoliubov transformation is applied to diagonalize the system in terms of fermions (variable a).

The scheme of the total operation is:

$$\mathcal{H}_{corr} = \mathcal{H}_1[\sigma] \longrightarrow \mathcal{H}_2[c] \xrightarrow{\mathcal{U}_{FT}} \mathcal{H}_3[b] \xrightarrow{\mathcal{U}_{Bog}} \mathcal{H}_4[a] = \tilde{\mathcal{H}}, \tag{4.1}$$

and the corresponding unitary operator is:

$$\mathcal{U} = \mathcal{U}_{Bog}\mathcal{U}_{FT}. \tag{4.2}$$

The advantage of this operator is that it can be simulated by a quantum circuit using only two qubit operations. We will present them for the XX and Ising Hamiltonians in this section.

Performing the unitary transformation on the disentangled Hamiltonian will lead to the strongly correlated Hamiltonian:

$$\mathcal{H}_{\mathrm{corr}} = \mathcal{U}\tilde{\mathcal{H}}\mathcal{U}^{\dagger}, \tag{4.3}$$

where

- $\tilde{\mathcal{H}} = \sum_i \omega_i \sigma_i^z$ is composed of strictly non interacting terms.

- $\mathcal{U}$ is the unitary transformation made of two qubit gates.

Thanks to this operation they can simulate any state of the different models. Each unitary transformation is specific to one model and to the number of qubits interacting in the system. Then the time evolution of one state or the thermal superposition of several states can be obtained using the following relations:

$$e^{-it\mathcal{H}_{XY}} = \mathcal{U}e^{-it\tilde{\mathcal{H}}}\mathcal{U}^{\dagger} \tag{4.4}$$

$$e^{-\beta\mathcal{H}_{XY}} = \mathcal{U}e^{-\beta\tilde{\mathcal{H}}}\mathcal{U}^{\dagger} \tag{4.5}$$

Concerning the quantum circuits which represent the unitary operations, they will be composed of three main types of two qubit operations performing the required Fourier transform and Bogoliubov transformation of the analytic work.

- The Fourier transform is composed of a fermionic $\overline{\mathrm{SWAP}}$ and an associated change of relative phase F_k:

$$\overline{\mathrm{SWAP}} = \begin{pmatrix} 1 & 0 & 0 & 0 \\ 0 & 0 & 1 & 0 \\ 0 & 1 & 0 & 0 \\ 0 & 0 & 0 & -1 \end{pmatrix} \quad F_k = \begin{pmatrix} 1 & 0 & 0 & 0 \\ 0 & \frac{1}{\sqrt{2}} & \frac{1}{\sqrt{2}} & 0 \\ 0 & \frac{e^{i\phi_k}}{\sqrt{2}} & -\frac{e^{i\phi_k}}{\sqrt{2}} & 0 \\ 0 & 0 & 0 & -e^{i\phi_k} \end{pmatrix}$$

The phase factor depends on the number n of qubits in the system:

$$e^{i\phi_k} = e^{-i2\pi k/n}. \tag{4.6}$$

There exists several F_k gates characterized by the index k. Each k corresponds to a different phase which depends on the analytic operation we have to perform and on the number of qubits n in the system.

- The Bogoliubov transformation is performed using the following matrix:

$$
B = \begin{pmatrix} \cos\theta & 0 & 0 & i\sin\theta \\ 0 & 1 & 0 & 0 \\ 0 & 0 & 1 & 0 \\ i\sin\theta & 0 & 0 & \cos\theta \end{pmatrix},
$$

where the angle θ depends on the external magnetic field λ: $\theta = \arctan(\lambda - \sqrt{1 + \lambda^2})$. This is needed to simulate the Ising model in an arbitrary transverse field.

In the next section we will see how to implement in Circuit QED these operations in the resonant regime. For this we will try to decompose the Fourier transform and the Bogoliubov operation in resonant steps with the help of an auxiliary level as already used for the CPHASE and iSWAP gates. The realization is not a trivial task and consitutes a new theoretical proposal for implementing gates in a fast way.

4.2   Physical implementation

It is known from the literature that it is possible to decompose any two qubit operation with a minimal set of universal gates, for instance the CNOT or CPHASE gates in addition to a finite number of local unitary operations. However this decomposition is not always the optimal one. The goal in this section is to perform the Fourier and Bogoliubov transformations fast although it may not correspond to a minimal number of operations. For this we will use the cavity qubit as mediator and a third excited level for one of the SCqubits. These were the tools already used in the previous sections to implement the two-qubit gates, the CPHASE, the iSWAP and the $\sqrt{\text{iSWAP}}$ gates, with resonant steps.

4.2.1   The $\overline{\text{SWAP}}$ gate

It can be written as:

$$
\overline{\text{SWAP}} = \text{SWAP} \otimes \text{CPHASE}. \tag{4.7}
$$

The CPHASE gate can be implemented in the resonant regime using the protocol described in the chapter 2. The SWAP can be decomposed as:

$$
\text{SWAP} = \text{CNOT}(1) * \text{CNOT}(2) * \text{CNOT}(1). \tag{4.8}
$$

Both CNOT gates can be decomposed with only resonant operations following the expressions

$$
\text{CNOT}(1) = \text{H}(2) * \text{CPHASE} * \text{H}(2), \quad \text{CNOT}(2) = \text{H}(1) * \text{CPHASE} * \text{H}(1). \tag{4.9}
$$

All these matrices are given in Appendix B. As we see, the $\overline{\text{SWAP}}$ is quite easy to implement because we already know how to implement the CPHASE and Hadamard gates with only resonant steps. It was the goal of the second chapter.

4.2.2   The F_k gates

These gates yield the phase associated with the Fourier transform. Their matrix can be decomposed as follows:

$$F_k = \begin{pmatrix} 1 & 0 & 0 & 0 \\ 0 & \frac{1}{\sqrt{2}} & \frac{1}{\sqrt{2}} & 0 \\ 0 & \frac{e^{i\phi_k}}{\sqrt{2}} & -\frac{e^{i\phi_k}}{\sqrt{2}} & 0 \\ 0 & 0 & 0 & -e^{i\phi_k} \end{pmatrix} = \begin{pmatrix} 1 & 0 & 0 & 0 \\ 0 & 1 & 0 & 0 \\ 0 & 0 & e^{i\phi_k+\pi} & 0 \\ 0 & 0 & 0 & e^{i\phi_k+\pi} \end{pmatrix} \begin{pmatrix} 1 & 0 & 0 & 0 \\ 0 & \frac{1}{\sqrt{2}} & \frac{1}{\sqrt{2}} & 0 \\ 0 & -\frac{1}{\sqrt{2}} & \frac{1}{\sqrt{2}} & 0 \\ 0 & 0 & 0 & 1 \end{pmatrix}.$$

The first matrix of the right-hand side of the equation corresponds to a local phase gate on the second qubit. This is a trivial operation which can be done fast. For the second we have to give a protocol to implement it in the resonant regime. We will first study what this second matrix does on a superposition of two qubits composed of two levels $\{|g_i\rangle, |e_i\rangle\}_{i=1,2}$:

$$\begin{pmatrix} 1 & 0 & 0 & 0 \\ 0 & \frac{1}{\sqrt{2}} & \frac{1}{\sqrt{2}} & 0 \\ 0 & -\frac{1}{\sqrt{2}} & \frac{1}{\sqrt{2}} & 0 \\ 0 & 0 & 0 & 1 \end{pmatrix} \begin{pmatrix} \alpha \\ \beta \\ \gamma \\ \delta \end{pmatrix} = \begin{pmatrix} \alpha \\ \frac{1}{\sqrt{2}}(\beta+\gamma) \\ \frac{1}{\sqrt{2}}(-\beta+\gamma) \\ \delta \end{pmatrix},$$

where $\alpha, \beta, \gamma, \delta$ are complex numbers.

The final state can be written:

$$\alpha |g_1 g_2\rangle + \frac{\beta}{\sqrt{2}}\Big(|g_1 e_2\rangle - |e_1 g_2\rangle\Big) + \frac{\gamma}{\sqrt{2}}\Big(|g_1 e_2\rangle + |e_1 g_2\rangle\Big) + \delta |e_1 e_2\rangle \tag{4.10}$$

It corresponds to the entanglement of the states $|g_1 e_2\rangle$ and $|e_1 g_2\rangle$.

We will show that it is possible to get this operation in five resonant steps. The experimental system is composed of two SCqubits with an auxiliary excited level, in a cavity which can contain 0 or 1 photon. The scheme is shown in Fig. 4.1. As for the CPHASE and iSWAP gates, we will present in a table the summary of all the steps so that one can get the general idea of the protocol Fig. 4.2. Then a detailed version is presented below.
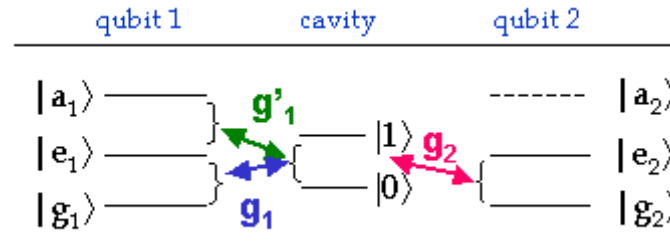

Figure 4.1: Scheme for the implementation of the Fourier transform operations.

The initial state is:

$$|\Psi_i\rangle = \Big(\alpha |g_1 g_2\rangle + \beta |g_1 e_2\rangle + \gamma |e_1 g_2\rangle + \delta |e_1 e_2\rangle\Big) \otimes |0\rangle. \tag{4.11}$$

Step	Required transitions	Coupling constant	Pulse
i) Mapping	$\{|g_2\rangle, |e_2\rangle\} \longrightarrow \{|0\rangle, |1\rangle\}$	**g₂**	π-pulse
ii) Shelving	$\{|e_1\rangle, |a_1\rangle\} \longleftrightarrow \{|0\rangle, |1\rangle\}$	**g'₁**	π-pulse
iii) Entanglement generation	$\{|e_1\rangle, |a_1\rangle\} \longleftrightarrow \{|0\rangle, |1\rangle\}$	**g₁**	$\pi/2$-pulse
iv) Back shelving	$\{|e_1\rangle, |a_1\rangle\} \longleftrightarrow \{|0\rangle, |1\rangle\}$	**g'₁**	$(-\pi)$-pulse
v) Back mapping	$\{|g_2\rangle, |e_2\rangle\} \longleftarrow \{|0\rangle, |1\rangle\}$	**g₂**	π-pulse

Figure 4.2: Protocol for the implementation of the Fourier transform operations.

The protocol described in Fig. 4.2 leads to the final state:

$$|\Psi_f\rangle = \left[\alpha\,|g_1g_2\rangle + \frac{\beta}{\sqrt{2}}\Big(|g_1e_2\rangle - |e_1g_2\rangle\Big) + \frac{\gamma}{\sqrt{2}}\Big(|g_1e_2\rangle + |e_1g_2\rangle\Big) + \delta\,|e_1e_2\rangle\right] \otimes |0\rangle, \quad (4.12)$$

which is exactly the desired state of Eq. 4.10. It constitutes the first theoretical proposal for the implementation of this non trivial gate in Circuit QED in a fast way.

Detailed protocol for the phase change associated to the Fourier transform

At the beginning the two qubits are in the cavity which contains zero photons. The initial state is:

$$|\Psi_0\rangle = \Big(\alpha\,|g_1g_2\rangle + \beta\,|g_1e_2\rangle + \gamma\,|e_1g_2\rangle + \delta\,|e_1e_2\rangle\Big) \otimes |0\rangle. \quad (4.13)$$

i) We want to use the cavity qubit as mediator.
For this we map the second qubit into the cavity by tuning on resonance the levels $\{|g_2\rangle, |e_2\rangle\}$ with the cavity $|0\rangle$ via the coupling constant g_2 for a π-quantum Rabi pulse. The resulting state is:

$$|\Psi_1\rangle = \Big(\alpha\,|g_10\rangle + \beta\,|g_11\rangle + \gamma\,|e_10\rangle + \delta\,|e_11\rangle\Big) \otimes |g_2\rangle. \quad (4.14)$$

ii) We want to shelve the population of the level $|e_1\rangle$ to the level $|a_1\rangle$ in order to be able to rotate the state $|g_1\rangle$ without touching other levels. For this we perform a qubit transfer by coupling the levels $\{|e_1\rangle, |a_1\rangle\}$ with the cavity via the coupling constant g'_1 for a π-quantum Rabi pulse. We get the state:

$$|\Psi_2\rangle = \Big(\alpha\,|g_10\rangle + \beta\,|g_11\rangle + \gamma\,|e_10\rangle + \delta\,|a_10\rangle\Big) \otimes |g_2\rangle. \quad (4.15)$$

iii) We want to generate an entanglement between the states $|g_1\rangle$ and $|e_1\rangle$ by tuning them on resonance with the cavity via the coupling constant g_1 for a $\pi/2$-quantum Rabi pulse. This is the main operation done by the Fourier transform gate as shown at the beginning of the paragraph.

The interaction Hamiltonian in this resonant coupling considering the rotating wave approximation is:

$$\mathcal{H}_{\text{int}}(t) = -\hbar g_1(\sigma_+ a e^{-i\phi} + \sigma_- a^\dagger, e^{i\phi}), \quad (4.16)$$

where ϕ is a well-defined experimental phase. The corresponding evolution operator is:

$$
\begin{aligned}
U_{\text{int}} \;=\; & \cos\left(g_1 t\sqrt{n+1}\right)|e_1\rangle\langle e_1| + \cos\left(g_1 t\sqrt{n}\right)|g_1\rangle\langle g_1| \\[4pt]
+ \; & ie^{-i\phi}\frac{\sin\left(g_1 t\sqrt{n+1}\right)}{\sqrt{n+1}}\, a\,|e_1\rangle\langle g_1| \\[4pt]
+ \; & ie^{i\phi}\, a^\dagger\,\frac{\sin\left(g_1 t\sqrt{n+1}\right)}{\sqrt{n+1}}\,|g_1\rangle\langle e_1|.
\end{aligned}
\tag{4.17}
$$

The state after a $\pi/2$-pulse looks like:

$$
\left[\alpha\,|g_10\rangle + \frac{\beta}{\sqrt{2}}\Big(|g_11\rangle + ie^{-i\phi}|e_10\rangle\Big) + \frac{\gamma}{\sqrt{2}}\Big(|g_11\rangle + ie^{i\phi}|e_10\rangle\Big) + \delta\,|a_10\rangle\right]\otimes|g_2\rangle.
\tag{4.18}
$$

To get what corresponds to the initial transformation described by the matrix, we have to choose the phase ϕ equal to $-\pi/2$.
So the state is:

$$
|\Psi_3\rangle = \left[\alpha\,|g_10\rangle + \frac{\beta}{\sqrt{2}}\Big(|g_11\rangle - |e_10\rangle\Big) + \frac{\gamma}{\sqrt{2}}\Big(|g_11\rangle + |e_10\rangle\Big) + \delta\,|a_10\rangle\right]\otimes|g_2\rangle.
\tag{4.19}
$$

iv) We have now the desired operation. We have thus to come back doing the inverse qubit transfer and the back mapping of the cavity qubit onto the second SCqubit to get the logical gate between the two SCqubits in the cavity. The inverse qubit transfer can be done by tuning on resonance the levels $\{|e_1\rangle, |a_1\rangle\}$ with the cavity via the coupling constant g_1' for a $(-\pi)$-quantum Rabi pulse. We get the state:

$$
|\Psi_4\rangle = \left[\alpha\,|g_10\rangle + \frac{\beta}{\sqrt{2}}\Big(|g_11\rangle - |e_10\rangle\Big) + \frac{\gamma}{\sqrt{2}}\Big(|g_11\rangle + |e_10\rangle\Big) + \delta\,|e_11\rangle\right]\otimes|g_2\rangle.
\tag{4.20}
$$

And the back mapping is performed by tuning on resonance the levels $\{|g_2\rangle, |e_2\rangle\}$ with the cavity via the coupling constant g_2 for a π-quantum Rabi pulse. The final state is:

$$
|\Psi_5\rangle = \left[\alpha\,|g_1g_2\rangle + \frac{\beta}{\sqrt{2}}\Big(|g_1e_2\rangle - |e_1g_2\rangle\Big) + \frac{\gamma}{\sqrt{2}}\Big(|g_1e_2\rangle + |e_1g_2\rangle\Big) + \delta\,|e_1e_2\rangle\right]\otimes|0\rangle.
\tag{4.21}
$$

This protocol allows us to implement the initial operation between two SCqubits inside the same cavity. We recall that it is described by the matrix:

$$
\begin{pmatrix}
1 & 0 & 0 & 0 \\
0 & \frac{1}{\sqrt{2}} & \frac{1}{\sqrt{2}} & 0 \\
0 & -\frac{1}{\sqrt{2}} & \frac{1}{\sqrt{2}} & 0 \\
0 & 0 & 0 & 1
\end{pmatrix}.
$$

We know at this stage how to perform the different F_k gates required in the quantum circuits for the XX and Ising models.

4.2.3 The Bogoliubov transformation

The effect of the matrix 4.1 on a general state of two qubits is:

$$
\begin{pmatrix}
\cos\theta & 0 & 0 & i\sin\theta \\
0 & 1 & 0 & 0 \\
0 & 0 & 1 & 0 \\
i\sin\theta & 0 & 0 & \cos\theta
\end{pmatrix}
\begin{pmatrix}
\alpha \\ \beta \\ \gamma \\ \delta
\end{pmatrix}
=
\begin{pmatrix}
\alpha\cos\theta + i\,\delta\sin\theta \\
\beta \\
\gamma \\
i\,\alpha\sin\theta + \delta\cos\theta
\end{pmatrix},
$$

where $\alpha, \beta, \gamma, \delta$ are complex numbers.

It corresponds to a rotation of the first and last states and can be written as:

$$
\alpha\left(\cos\theta\,|g_1g_2\rangle + i\,\sin\theta\,|e_1e_2\rangle\right) + \beta\,|g_1e_2\rangle + \gamma\,|e_1g_2\rangle + \delta\left(i\,\sin\theta\,|g_1g_2\rangle + \cos\theta\,|e_1e_2\rangle\right). \tag{4.22}
$$

This operation looks like the Fourier transform studied before, but the entanglement is here between the states $|g_1g_2\rangle$ and $|e_1e_2\rangle$ and with a free angle θ instead of an entanglement between the states $|g_1e_2\rangle$ and $|e_1g_2\rangle$ implemented with a $\pi/2$-pulse. So we can almost use the same protocol as for the Fourier transform gate but we have to rotate the first qubit before entangling its first two levels. The rotation of the first qubit will be done by sending a classical field in resonance with its transition frequency with a coupling constant Ω_R.
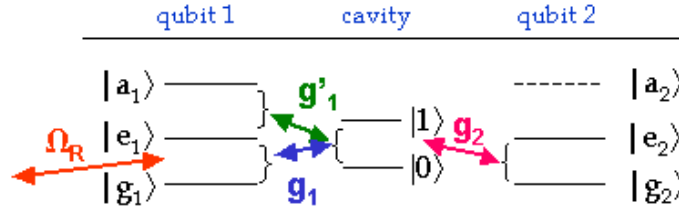
The experimental setup is described in Fig. 4.3.

Figure 4.3: Scheme for the implementation of the Bogoliubov transformation.

The initial state is:

$$
|\Psi_i\rangle = \left[\alpha\,|g_1g_2\rangle + \beta\,|g_1e_2\rangle + \gamma\,|e_1g_2\rangle + \delta\,|e_1e_2\rangle\right]\otimes|0\rangle. \tag{4.23}
$$

After performing the operations described in the table Fig. 4.4 on the initial state, we finally obtain:

$$
\begin{aligned}
|\Psi_f\rangle &= \left[\alpha\left(\cos\theta\,|g_1g_2\rangle + i\,\sin\theta\,|e_1e_2\rangle\right) + \beta\,|g_1e_2\rangle + \right. \\
&\quad + \left. \gamma\,|e_1g_2\rangle + \delta\left(\cos\theta\,|e_1e_2\rangle + i\,\sin\theta\,|g_1g_2\rangle\right)\right]\otimes|0\rangle. \tag{4.24}
\end{aligned}
$$

which is exactly the desired state.

Step	Required transitions	Coupling constant	Pulse
i) Mapping	$\{|g_2\rangle, |e_2\rangle\} \longrightarrow \{|0\rangle, |1\rangle\}$	g_2	π-pulse
ii) Rotation of qubit 1	$\{|g_1\rangle, |e_1\rangle\} \longleftrightarrow \{|0\rangle, |1\rangle\}$	Ω_R	π-pulse
iii) Shelving	$\{|e_1\rangle, |a_1\rangle\} \longleftrightarrow \{|0\rangle, |1\rangle\}$	g'_1	π-pulse
iv) Entanglement	$\{|g_1\rangle, |e_1\rangle\} \longleftrightarrow \{|0\rangle, |1\rangle\}$	g_1	2θ-pulse
v) Back shelving	$\{|e_1\rangle, |a_1\rangle\} \longleftrightarrow \{|0\rangle, |1\rangle\}$	g'_1	$(-\pi)$-pulse
vi) Back rotation	$\{|g_1\rangle, |e_1\rangle\} \longleftrightarrow \{|0\rangle, |1\rangle\}$	Ω_R	π-pulse
vii) Back mapping	$\{|g_2\rangle, |e_2\rangle\} \longleftarrow \{|0\rangle, |1\rangle\}$	g_2	π-pulse

Figure 4.4: Protocol for the Bogoliubov transformation.

Detailed protocol for the Bogoliubov transformation

The initial state is:

$$|\Psi_0\rangle = \left(\alpha |g_1g_2\rangle + \beta |g_1e_2\rangle + \gamma |e_1g_2\rangle + \delta |e_1e_2\rangle\right) \otimes |0\rangle. \tag{4.25}$$

i) We want to use the cavity as a mediator for the operation.
For this we map the second qubit into the cavity by tuning on resonance the levels $\{|g_2\rangle, |e_2\rangle\}$ with the cavity $|0\rangle$ via the coupling constant g_2 for π-quantum Rabi pulse. The resulting state is:

$$|\Psi_1\rangle = \left(\alpha |g_10\rangle + \beta |g_11\rangle + \gamma |e_10\rangle + \delta |e_11\rangle\right) \otimes |g_2\rangle. \tag{4.26}$$

ii) We rotate the first qubit by sending a classical field on it in resonance between levels $\{|g_1\rangle, |e_1\rangle\}$ with the coupling constant Ω_R for a π-pulse. The general phase of the rotation ϕ must be set to $-\pi/2$. This leads to the transformation:

$$|g_1\rangle \longrightarrow |e_1\rangle, \tag{4.27}$$
$$|e_1\rangle \longrightarrow -|g_1\rangle. \tag{4.28}$$

The state reads:

$$|\Psi_2\rangle = \left(\alpha |e_10\rangle + \beta |e_11\rangle - \gamma |g_10\rangle - \delta |g_11\rangle\right) \otimes |g_2\rangle. \tag{4.29}$$

iii) We can perform now the steps ii) and iii) of the Fourier transform operation detailed in the last paragraph corresponding to the qubit transfer of level $|e_1\rangle$ to level $|a_1\rangle$ and then the entanglement generation of the states $|g_1g_2\rangle$ and $|e_1e_2\rangle$. The qubit transfer leads to the state:

$$|\Psi_3\rangle = \left(\alpha |e_10\rangle + \beta |a_10\rangle - \gamma |g_10\rangle - \delta |g_11\rangle\right) \otimes |g_2\rangle. \tag{4.30}$$

For the entanglement generation we tune on resonance the levels $\{|g_1\rangle, |e_1\rangle\}$ with the cavity via the coupling constant g_1 choosing the global phase ϕ equal to π for a 2θ-quantum

Rabi pulse where θ is a function of the strength of the external magnetic field. The state is:

$$
\begin{aligned}
|\Psi_4\rangle \;=\; & \Big[-\gamma\,|g_1 0\rangle - \delta\Big(\cos\theta|g_1 1\rangle - i\,\sin\theta\,|e_1 0\rangle\Big) + \\
& + \;\alpha\Big(\cos\theta\,|e_1 0\rangle - i\,\sin\theta\,|g_1 1\rangle\Big) + \beta\,|a_1 0\rangle\Big] \otimes |g_2\rangle.
\end{aligned}
\tag{4.31}
$$

We have now the desired entanglement depending on the parameter θ. As for the Fourier transform we have to do the first operations in the other direction in order to get finally the gate between the two SCqubits in the cavity. For this we implement the following steps.

v) We perform the inverse qubit transfer by tuning on resonance the levels $\{|e_1\rangle, |a_1\rangle\}$ with the cavity via the coupling constant g'_1 for a $(-\pi)$-quantum Rabi pulse. The state is:

$$
\begin{aligned}
|\Psi_5\rangle \;=\; & \Big[-\gamma\,|g_1 0\rangle - \delta\Big(\cos\theta\,|g_1 1\rangle - i\,\sin\theta\,|e_1 0\rangle\Big) + \\
& + \;\alpha\Big(\cos\theta\,|e_1 0\rangle - i\,\sin\theta\,|g_1 1\rangle\Big) + \beta\,|e_1 1\rangle\Big] \otimes |g_2\rangle.
\end{aligned}
\tag{4.32}
$$

vi) We rotate back the first qubit by sending a classical field on it in resonance between levels $\{|g_1\rangle, |e_1\rangle\}$ with the coupling constant Ω_R for a π-pulse. The general phase of the rotation ϕ must be taken equal to $-\pi/2$. The transformation will thus correspond to:

$$
|g_1\rangle \;\longrightarrow\; -|e_1\rangle, \tag{4.33}
$$

$$
|e_1\rangle \;\longrightarrow\; |g_1\rangle. \tag{4.34}
$$

The state becomes:

$$
\begin{aligned}
|\Psi_6\rangle \;=\; & \Big[\gamma\,|e_1 0\rangle + \delta\Big(\cos\theta\,|e_1 1\rangle + i\,\sin\theta\,|g_1 0\rangle\Big) + \\
& + \;\alpha\Big(\cos\theta\,|g_1 0\rangle + i\,\sin\theta\,|e_1 1\rangle\Big) + \beta\,|g_1 1\rangle\Big] \otimes |g_2\rangle.
\end{aligned}
\tag{4.35}
$$

vii) We map back the cavity qubit onto the second SCqubit by tuning on resonance the levels $\{|g_2\rangle, |e_2\rangle\}$ with the cavity via the coupling constant g_2 for a π-quantum Rabi pulse. The final state is:

$$
\begin{aligned}
|\Psi_7\rangle \;=\; & \Big[\gamma\,|e_1 g_2\rangle + \delta\Big(\cos\theta\,|e_1 e_2\rangle + i\,\sin\theta\,|g_1 g_2\rangle\Big) + \\
& + \;\alpha\Big(\cos\theta\,|g_1 g_2\rangle + i\,\sin\theta\,|e_1 e_2\rangle\Big) + \beta\,|g_1 e_2\rangle\Big] \otimes |0\rangle.
\end{aligned}
\tag{4.36}
$$

Thanks to this expression we see that it is exactly what the Bogoliubov operation does. This can be rewritten as:

$$
\begin{aligned}
|\Psi_f\rangle \;=\; & \Big[\alpha\Big(\cos\theta\,|g_1 g_2\rangle + i\,\sin\theta\,|e_1 e_2\rangle\Big) + \beta\,|g_1 e_2\rangle + \\
& + \;\gamma\,|e_1 g_2\rangle + \delta\Big(\cos\theta\,|e_1 e_2\rangle + i\,\sin\theta\,|g_1 g_2\rangle\Big)\Big] \otimes |0\rangle.
\end{aligned}
\tag{4.37}
$$

Summary

In this chapter, we implemented non trivial two-qubit operations that could be used to simulate strongly correlated Hamiltonians such as the Hamiltonians for the XX model and the Ising model in a transverse magnetic field in one dimension. We achieved the implementation using a finite number of states and moreover purely resonant fast gates. From an experimental point of view it is an important issue due to the decoherence of all actual qubits. The use of the cavity as mediator and three-level physics were the key tools for this fast implementation.

4.3   Back to one-way quantum computing

An extension of the Ising model will be to build a cluster state which is required for one-way quantum computing as explained in the last chapter. If the initial state is composed of a number N of qubits in a superposition state $\frac{1}{\sqrt{2}}(|0\rangle + |1\rangle)$, then applying the evolution operator of the Ising Hamiltonian in one dimension during a time $gt = \pi$ on this initial state will lead to a cluster state.
The evolution operator of the Ising model is given by [33]:

$$U_{\text{Ising}} = \exp[-igt \sum_a (\frac{1 + \sigma_z^a}{2})(\frac{1 - \sigma_z^a}{2})].$$ (4.38)

And the cluster state is defined as:

$$|\phi_N\rangle = \frac{1}{2^{N/2}} \bigotimes_{a=1}^{N} (|0\rangle_a + |1\rangle_a \sigma_z^{a+1}).$$ (4.39)

The great advantage of the Ising model is that all operations commute. That means that if we are able to implement it in a physical architecture, it will be possible to generate theoretically a cluster state in one dimension extremely fast.

However one-way quantum computing requires a cluster state in two dimensions. Theoretically it is possible to do it by implementing an interaction of the Ising type between each neighbour qubits. As a possible outlook, we conjecture about the possibility of building a two-dimensional cluster state with the simulation techniques discussed in [37].

Conclusion

We presented the novel field of Circuit QED and the actual devices used in the research. We detailed the four main kinds of qubits considered as artificial atoms, the one-dimensional resonator which plays the role of the cavity and the 2D-cavity grid made of $N \times N$ resonators where qubits are situated at the crossing points between two cavities. In this work we considered this recently proposed architecture and tried to exploit its advantages to optimize in time the implementation of universal gates required for quantum computing and the realization of protocols to get multiqubit entangled states. In fact the time needed for operations and protocols is a crucial issue for quantum computing because of the decoherence of the qubits despite the recent improvements.

Then we focused on the realization in a fast way of one- and two-qubit operations which can form a set of universal operations: the Hadamard, the CPHASE, the iSWAP and $\sqrt{\text{iSWAP}}$ gates. To reach the goal of a fast implementation, we used different tools.
For the Hadamard gate which corresponds to a rotation in the Bloch sphere, we derived an alternative expression which uses only the x and y rotations instead of the x and z rotations. Indeed the latter corresponds in our setup to an ac-Stark shift and is slow as consequence. Moreover we detailed the experimental realization of this gate by explaining how the required pulses can be produced with a microwave generator.
For the two qubit gates, we worked with two qubits situated in a same resonator. To implement the operations in a fast way, we considered the cavity-qubit as a mediator for the operation and we used an auxiliary level for one of the qubits. Three-level physics is a tool aready known in quantum optics and trapped ions but it has never been used before for the purposes of quantum gate implementation in Circuit QED. We showed with a simulation that it seems reasonable to use this third level in a superconducting qubit: it looks possible to find values for the key parameters of the qubits for which the anharmonicity of the energy levels is strong enough to prevent qubit operations from exciting other transitions in the system. This allowed us to develop specific protocols using only resonant steps for the CPHASE, iSWAP and $\sqrt{\text{iSWAP}}$ gates. They are much faster than realizations in the off-resonant regimes when supposing a large qubit-resonator detuning. The proposed set of fast gates forms a useful toolbox for implementing algorithms and protocols of quantum computing in Circuit QED. Direct applications are the subject of chapters 3 and 4.

As first example, we concentrated on generating a multiqubit entangled state required for a one-way quantum computer: the cluster state. One-way quantum computing is an alternative scalable model to standard quantum computing where the amount of entanglement for the full computation is provided by the initial cluster state. We developed a protocol to implement this cluster state in two dimensions with N^2 superconducting qubits in a time

linear with N using the fast resonant gates of chapter 2. Thus we achieved the optimization in time of the realization of a multiqubit entangled state in Circuit QED.
A second application is the simulation of strongly correlated systems like the XX and Ising models. The theoretical idea is to cast the strongly correlated Hamiltonian into a local term Hamiltonian by performing a unitary transformation. The main advantage of this transformation is that it can be simulated by quantum circuits composed of a finite number of non trivial two-qubit gates. We developed protocols to implement in a fast way these non trivial gates in Circuit QED. In this case, we used again the cavity as mediator and an auxiliary excited level for one superconducting qubit.

Summarizing, we achieved the implementation in Circuit QED of most important one- and two-qubit gates for quantum computing in a fast way using as main tools resonant operations and an auxiliary excited level for each superconducting qubit. We showed that this toolbox of fast resonant operations can be useful for instance to optimize in time the realization of a cluster state which is a multiqubit entangled state. Furthermore using three-level physics again, we proposed protocols to implement non trivial two-qubit gates required for specific quantum circuits that can simulate strong correlated models in one dimension like the Ising model in a transverse magnetic field.
We could think about the gates and quantum circuits needed for the simulation of the Ising model in two dimensions. This could enable the realization of a cluster of N^2 qubits in two dimensions with a circuit model and improve the realization time. Another ongoing possibility is the use of optimal control techniques for improving on the number and the time of involved operations.

Appendix A

Three-level physics

In this appendix, we will explain the program written in Mathematica in order to justify the use of an auxiliary level for one superconducting qubit in our protocols for the implementation of fast gates in Circuit QED. Indeed there are several conditions for this use. First we have to be sure that a third excited level exists in the considered qubit: the levels considered for the two-level system are different, according to the type of qubits we consider. They depend on the energy potential characteristic of each qubit. Then, the anharmonicity of the energy levels in this potential has to be strong enough in order to be able to choose the transition frequencies we want to work with and not other ones.

The aim of the Mathematica program is to show the energy levels for each qubit as a function of their key parameters: the ratio E_J/E_C, where E_J is the Josephson energy and E_C the coupling energy, and the charge gate N_g. The ratio defines the type of qubit (charge, flux, phase or transmon qubits). Usually we aim at working near the degeneracy point N_g in order to reduce the decoherence of the qubit. So near this value we will calculate the levelspacing between the first four levels and see whether there exist values for the ratio E_J/E_C for which the anharmonicity of the levels is strong enough. Or, putting it differently, we will check whether the transition frequencies are different enough from one another. If such values exist, then it seems to be reasonable to use a superconducting qubit with an auxiliary excited level and to profit from the three-level physics techniques.
Let us mention that we used the Hamiltonian describing the charge and transmon qubits so the results are only valid for these two kinds of qubits. A similar program for the phase and flux qubits would have to be done in order to extend these results.

We will now present the program in more detail. To plot the energy levels we had first to consider the Hamiltonian of the qubit in the basis of the number of charge on the island $|N\rangle$ and to look for its eigenvalues and eigenvectors.

$$H_Q = 4E_C \sum_N (N - N_g)^2 |N\rangle\langle N| - \frac{E_J}{2} \sum_N \left(|N+1\rangle\langle N| + |N\rangle\langle N+1| \right) \qquad \text{(A.1)}$$

We defined it as a function of the ration E_J/E_C denoted $ejec$, the gate charge N_g denoted NG, and the maximum number of Cooper pairs in the island we want to consider, denoted $maxN$. Then we normalized these energies by subtracting the energy of the ground state. The ratio $ejec$ has to take values from 0 to 50 to cover the range of the charge and transmon qubits,

this is given in *ejecval* and the gate charge can cover the number of values given in *ngval*. We then defined a table which contains all the values of the eigenenergies corresponding to each ratio of *ejecval* and for all gate charges of *ngval*. To visualize the anharmonicity, we define the level spacing between the first four energy levels. Indeed we need the first three for our protocols but we want to be sure that when we tune to resonance the transition frequency between the second and third levels, we do not risk to touch the transition frequency between the third and fourth levels. Finally, we can set an additional parameter δ which defines the minimum degree of anharmonicity we want. A table gives us the values for *ejec* and *ng* for which the condition is verified. These values constitute the proof that it is reasonable to think about the use of this third level at least in the charge and transmon qubits.

Appendix B

Complement to two-qubit gates

In this appendix we will present the matrices corresponding to some basic two-qubits gates mentioned in the chapter 4. They are useful to decompose the fermionic SWAP gate $\overline{\text{SWAP}}$ into gates which can be implemented in the resonant regime. We remember the matrix form of the $\overline{\text{SWAP}}$ gate and its possible decomposition.

$$\overline{\text{SWAP}} = \begin{pmatrix} 1 & 0 & 0 & 0 \\ 0 & 0 & 1 & 0 \\ 0 & 1 & 0 & 0 \\ 0 & 0 & 0 & -1 \end{pmatrix}$$

It can be written as:

$$\overline{\text{SWAP}} = \text{SWAP} \otimes \text{CPHASE}. \tag{B.1}$$

Thanks to our work in chapter 2, we know how to implement the CPHASE gate in a fast way. So we have to see how the SWAP gate can be implemented in the resonant regime too. The SWAP can be decomposed as:

$$\text{SWAP} = \text{CNOT}(1) * \text{CNOT}(2) * \text{CNOT}(1). \tag{B.2}$$

Both CNOT gates can be decomposed with only resonant operations following the expressions:

$$\text{CNOT}(1) = \text{H}(2) * \text{CPHASE} * \text{H}(2) \quad \text{CNOT}(2) = \text{H}(1) * \text{CPHASE} * \text{H}(1). \tag{B.3}$$

The matrix form of all these new introduced gates is given in the following.

- $H(1) = H_1 \otimes \mathbb{I}_2$: qubit1 as target-qubit; qubit2 as control-qubit

$$H(1) = \frac{1}{\sqrt{2}} \begin{pmatrix} 1 & 0 & 1 & 0 \\ 0 & 1 & 0 & 1 \\ 1 & 0 & -1 & 0 \\ 0 & 1 & 0 & -1 \end{pmatrix}$$

- $H(2) = \mathbb{I}_1 \otimes H_2$: qubit2 as target-qubit; qubit1 as control-qubit

$$H(2) = \frac{1}{\sqrt{2}} \begin{pmatrix} 1 & 1 & 0 & 0 \\ 1 & -1 & 0 & 0 \\ 0 & 0 & 1 & 1 \\ 0 & 0 & 1 & -1 \end{pmatrix}$$

- The controlled-phase gate (CPHASE)

$$\text{CPHASE} = \begin{pmatrix} 1 & 0 & 0 & 0 \\ 0 & 1 & 0 & 0 \\ 0 & 0 & 1 & 0 \\ 0 & 0 & 0 & -1 \end{pmatrix}$$

- The CNOT(1) gate

$$\text{CNOT}(1) = \begin{pmatrix} 1 & 0 & 0 & 0 \\ 0 & 1 & 0 & 0 \\ 0 & 0 & 0 & 1 \\ 0 & 0 & 1 & 0 \end{pmatrix}$$

This operation can be decomposed as:

$$\text{CNOT}(1) = H(2) * \text{CPHASE} * H(2). \tag{B.4}$$

- The CNOT(2)

$$\text{CNOT}(2) = \begin{pmatrix} 1 & 0 & 0 & 0 \\ 0 & 0 & 0 & 1 \\ 0 & 0 & 1 & 0 \\ 0 & 1 & 0 & 0 \end{pmatrix}$$

This operation can be decomposed as:

$$\text{CNOT}(2) = H(1) * \text{CPHASE} * H(1). \tag{B.5}$$

In conclusion using the protocols developed in chapter 2 for the Hadamard and CPHASE gates, we know how to implement the fermionic SWAP in the resonant regime.

Bibliography

[1] M. Tinkham, *Introduction to superconductivity*, McGraw-Hill International Editions, second edition (1996).

[2] J.M. Raimond, M. Brune and S. Haroche, *Manipulating quantum entanglement with atoms and photons in a cavity*, Rev. Mod. Phys. **73**, 565 (2001).

[3] A. Wallraff, D.I. Schuster, A. Blais, L. Frunzio, R.S. Huang, J. Majer, S. Kumar, S.M. Girvin and R.J. Schoelkopf, *Strong coupling of a single photon to a superconducting qubit using circuit quantum electrodynamics*, Nature **400** (2004).

[4] I. Chiorescu, P. Bertet, K. Semba, Y. Nakamura, C.J.P.M. Harmans and J.E. Mooij, *Coherent dynamics of a flux qubit coupled to a harmonic oscillator*, Nature **431**, 159 (2007).

[5] Y. Makhlin, G. Schön and A. Shnirman, *Quantum state engineering with Josephson-junction devices*, Rev. Mod. Phys. **73**, 357-400 (2004).

[6] J.M. Martinis and K. Osbourne, *Superconducting qubits and the physics of Josephson junctions*, Les Houches conference proceedings, cond-mat/0402415 (2004).

[7] M.H. Devoret and J.M. Martinis, *Implementing qubits with superconducting integrated circuits*, Quantum Information Vol.3, N.1 (2004).

[8] I. Cirac and P. Zoller, *A scalable quantum computer with ions in an array of microtraps*, Nature **404**, 579 (2000).

[9] D. Kielpinski, C. Monroe and D.J. Wineland, *Architecture for a large-scale ion-trap quantum computer*, Nature **417**, 709 (2002).

[10] I. Wilson-Rae and A. Imamoglu, *Quantum dot cavity-QED in the presence of strong electron-phonon interactions*, Phys. Rev. B **65**, 235311 (2002).

[11] J.M. Taylor, H.-A. Engel, W. Dür, A. Yacoby, C.M. Marcus, P. Zoller and M.D. Lukin, *Fault-tolerant architecture for quantum computation using electrically controlled semiconductor spins*, Nature Physics **1**, 177 (2005).

[12] A. Blais, R.S. Huang, A. Wallraff, S.M. Girvin and R.J. Schoelkopf, *Cavity quantum electrodynamics for superconducting electrical circuits: An architecture for quantum computation*, Phys. Rev. A **69**, 062320 (2004).

[13] J.Q. You and F. Nori, *Superconducting Qubits and Quantum Information*, Physics Today, November (2005).

[14] F. Deppe, M. Mariantoni, E.P. Menzel, S. Saito, K. Kakuyanagi, H. Tanaka, T. Meno, K. Semba, H. Takayanagi and R. Gross, *Phase-Coherent Dynamics of a Superconducting Flux Qubit with Capacitive-Bias Readout*, cond-mat/0710.4455v1 (2007).

[15] M. Steffen, M. Ansmann, R. McDermott, N. Katz, R.C. Bialczak, E. Lucero, M. Neeley, E.M. Weig, A.N. Cleland and J.M. Martinis, *State Tomography Of Capacitively Shunted Phase Qubits with High Fidelity*, Phys. Rev. Lett. **97**, 050502 (2006).

[16] M.A. Sillanpää, J.I. park and R.W. Simmonds, *Coherent quantum state storage and transfer between two phase qubits via a resonant cavity*, Nature **449**, 438 (2007).

[17] J. Koch, T.M. Yu, J. Gambetta, A.A. Houck, D.I. Schuster, J. Majer, A. Blais, M.H. Devoret, S.M. Girvin and R.J. Schoelkopf, *Charge-insensitive qubit design derived from the Cooper pair box*, Phys. Rev. A **76**, 042319 (2007).

[18] F. Helmer, M. Mariantoni, A.G. Fowler, J. von Delft, E. Solano and F. Marquardt, *Two-dimensional cavity grid for scalable quantum computation with superconducting qubits*, cond-mat/0706.3625v1 (2007).

[19] O. Scully and M.S. Zubairy, *Quantum Optics*, Cambridge University Press, Fifth edition (2006).

[20] S. Haroche and J.M. Raymond, *Exploring the quantum: Atoms, Cavities and Photons*, Oxford University Press, First edition (2006).

[21] M.A. Nielsen and I.L. Chuang, *Quantum Computation and Quantum Information*, Cambridge University Press, Fifth edition (2004).

[22] D.A. Long, *Raman spectroscopy*, McGraw-Hill International Editions (1977).

[23] D. Leibfried, R. Blatt, C. Monroe and D. Wineland, *Quantum dynamics of single trapped atoms*, Rev. Mod. Phys. **75**, 281-324 (2003).

[24] S. Nussmann, K. Murr, M. Hijlkema, B. Weber, A. Kuhn and G. Rempe, *Vacuum-stimulated cooling of single atoms in three dimensions*, Nature Physics **1**, 122 (2005).

[25] J. McKeever, A. Boca, A.D. Boozer, J.R. Buck and H.J. Kimble, *Experimental realization of a one-atom laser in the regime of strong coupling*, Nature **425**, 268 (2003).

[26] M. Mariantoni, M.J. Storcz, F.K. Wilhelm, W.D. Olivier, A. Emmert, A. Marx, R. Gross, H. Christ and E. Solano, *On-chip microwave Fock states and quantum homodyne measurements*, cond-mat/0509737v2.

[27] J. Siewert and T. Brandes, *Applications of adiabatic passage in solid-state devices*, cond-mat/0506412v1.

[28] G. Nogues, A. Rauschenbeutel, S. Osnaghi, M. Brune, J.M. Raimond and S. Haroche, *Seeing a single photon without destroying it*, Nature **400**, 239 (1999).

[29] A. Blais, J. Gambetta, A. Wallraff, D.I. Schuster, S.M. Girvin, M.H. Devoret and R.J. Schoelkopf, *Quantum-information processing with circuit quantum electrodynamics*, Phys. Rev. A **75**, 032329 (2007).

[30] J. Majer, J.M. Chow, J.M. Gambetta, J. Koch, B.R. Johnson, J.A. Schreier, L. Frunzio, D.I. Schuster, A.A. Houck, A. Wallraff, A. Blais, M.H. Devoret, S.M. Girvin and R.J. Schoelkopf, *Coupling superconducting qubits via a cavity bus*, Nature **449**, 443 (2007).

[31] N. Schuch and J. Siewert, *Natural two-qubit gate for quantum computation using the XY interaction*, Phys. Rev. A **67**, 032301 (2003).

[32] R. Raussendorf and H.J. Briegel, *A one-way quantum computer*, Phys. Rev. Lett. **86**, 5188 (2001).

[33] R. Raussendorf and H.J. Briegel, *Persistent entanglement in arrays of interacting particles*, Phys. Rev. Lett. **86**, 910 (2001).

[34] W. Dür, G. Vidal and J.I. Cirac, *Three qubits can be entangled in two inequivalent ways*, Phys. Rev. A **62**, 062314 (2000).

[35] L. Lamata, J. Leon, D. Salgado and E. Solano, *Inductive entanglement classification of four qubits under stochastic local operations and classical communication*, Phys. Rev. A **75**, 022318 (2007).

[36] V. Coffman, J. Kundu and W.K. Wooters, *Distributed entanglement*, Phys. Rev. A **61**, 052306 (2000).

[37] F. Verstraete, I. Cirac and J.I. Latorre, *Quantum circuits for strongly correlated quantum system*, unpublished (2007).

Acknowledgments